Bioprinting 32 (2023) e00274

Contents lists available at ScienceDirect

Bioprinting

journal homepage: www.sciencedirect.com/journal/bioprinting

Design aspects and characterization of hydrogel-based bioinks for extrusion-based bioprinting

Jennika Karvinen *, Minna Kellomäki

Biomaterials and Tissue Engineering Group, Faculty of Medicine and Health Technology and BioMediTech Institute, Tampere University, Tampere, Finland

ARTICLE INFO

Keywords:
3D-bioprinting
Hydrogel
Printability
Characterization

ABSTRACT

3D-bioprinting has become a valid technique for tissue and organ regeneration, as the printing of living cells is allowed while the hydrogel-based ink material provides them mechanical and structural support. Self-healing shear-thinning hydrogel inks can be considered most promising ink materials for extrusion-based bioprinting (EBB), because the ink can be extruded due to the decrease in viscosity under shear, and self-healed after removing the shear, which ensures safe printing of cells and shape fidelity after bioprinting. To achieve the best final bioprinting result, some printing technique, ink material and biological aspects of bioprinting need to be considered. In addition, the versatile characterization of pre- and post-printing properties of the inks helps to improve the final bioprinted constructs. However, despite the great advances in 3D-bioprinting, ink related challenges such as opposing characteristics, and lack of controllable micro-environment, or technological challenges such as the need to increase printing speed and print resolution must be resolved. In terms of ink characterization, more standardization is also needed. In addition, the computational modeling would help to improve the performance of the bioprinted construct. Thus, the future of 3D-bioprinting is going towards larger multifunctional tissue/organ constructs with multi-scale vascularization and innervation. Multiple printing techniques are probably combined, but also completely new techniques are needed. Further, multimaterial printing would enable heterogeneity and gradients to the construct. On the other hand, using 4D-bioprinting, the dynamic nature of complex organs could be added to the construct. By combining bioprinting with microphysiological platforms (tissue- or organ-on-a-chip systems) the development of functional tissues and organs intended for implantation would go forward. The translation of EBB into clinical practice is still in the early stages, but EBB has a great potential in regenerative medicine after the challenges, such as biomimicry, reproducibility or up-scaling related issues have been overcome. In this review, the design aspects related to extrusion-based bioprinting technique, the property requirements for ideal bioink, the biological aspects of 3D-bioprinting, and the characterization of the pre- and post-printing properties of bioinks are presented. Also, the challenges and future prospects of 3D-bioprinting are discussed.

1. Introduction

Aging population and prolonged life expectancy have led to increasing demand of tissue and organ transplants, which have led to a continuous lack of them [1,2]. Further, death of patients and possible post-operative graft rejections have led to need of alternative solutions [3]. Synthetic biomaterials, possibly together with patient's own cells, are potential solutions for the problem [3]. Despite the great advances in tissue engineering already, it has been noticed that the regeneration of soft tissue i.e. creation of its three dimensional (3D) structure, is difficult due to its viscosity, flexibility and high elasticity [2,4]. Conventional techniques such as electrospinning or injection molding have limited control over the scaffold composition, architecture or pore shape causing a demand for alternative techniques [2]. 3D-(bio)printing has became an eligible technique to overcome those limitations [4]. Patient's own cells can be used for construction of tissues and organs with the help of computer-aided design (CAD) (pre-processing) and computer-aided manufacturing creating 3D structures in a layer-by-layer fashion (processing) [3,5]. The transplantation of the construct can be done after a period of *in vitro* maturation, or the construct is used for *in vitro* analysis (post-processing) [6].

Four printing techniques, i.e. extrusion-based, inkjet-based, laser

* Corresponding author.
E-mail address: jennika.karvinen@tuni.fi (J. Karvinen).

https://doi.org/10.1016/j.bprint.2023.e00274
Received 18 January 2023; Received in revised form 18 March 2023; Accepted 5 April 2023
Available online 15 April 2023

assisted and stereolithography are widely used for bioprinting [7]. Also, bioprinting techniques can be divided according to the need: sacrificial bioprinting (produces vascular network simulating interconnected hollow channels), embedded bioprinting (3D structures are directly printed) and multi-material bioprinting (produces complex tissues containing multiple cell types, ECMs, and/or gradients) [8]. The bioprinting types on the other hand can be divided into five types (Table 1) [9,10]: direct bioprinting, in-process crosslinking, post-processing crosslinking, indirect bioprinting, and hybrid bioprinting.

Bioink refers to specialized cells (e.g. stem cells), and hydrogel-based "biopaper" that provides them mechanical and structural support [11]. More precisely, bioink is a material (ink formulation) that is printed allowing the printing of living cells [2]. Hydrogels are suitable materials for 3D-bioprinting due to their similarity to ECM [12]. Hydrogels can facilitate cell adhesion and migration and matrix remodeling in 3D environment, which is needed for the normal development of functional tissues [1]. Self-healing hydrogels, inspired by the healing ability of body *in vivo* (e.g. wound healing), are even more eligibly than traditional hydrogels [12], because unlike traditional hydrogels, they are able to recover the broken bonds of the network after damage (e.g. extrusion), i.e. their initial structure, properties and functionality can be restored from micro-to macroscale, ideally rapidly and repeatedly [12–14]. Further, shear-thinning property of some hydrogels makes them suitable materials for 3D-(bio)printing applications, i.e. the preformed hydrogel can be injected by applying a shear stress during printing which lowers the viscosity of gel and makes it flow (under shear), and after removing the shear the hydrogel quickly self-heals and restores its rigidity [15–17].

For 3D-bioprinting of tissue constructs printable, elastic and high-strength hydrogel materials would be ideal inks, since many conventional hydrogels cannot meet the handling and soft/elastic tissue requirements due to their mechanical weakness and brittleness [18].

Table 1
Bioprinting types [9,10].

#	Type	Properties
1	Direct bioprinting	Materials are directly printed in a layer-by-layer or point-by-point manner to generate 3D structures with pre-determined configurations and shapes. Multiple cell types and materials can be deposited in order to create constructs with *in vivo* mimicking heterogeneity and improved reproducibility.
2	In-process crosslinking	Rapid gelation mechanisms of hydrogels are used. The hydrogel precursor can be deposited into crosslinker path, or the hydrogel precursor and crosslinker can be coaxially extruded with modified extrusion head. Third option is to design the toolpath of printer for the sequential deposition of hydrogel precursor and crosslinker.
3	Post-processing crosslinking	Multiple crosslinking mechanisms with mixture of hydrogels are used. In the mixture, primary material is for the improvement of shape fidelity and printability during printing, whereas secondary material provides structural fidelity by undergoing crosslinking after printing.
4	Indirect bioprinting	Build/support configuration is used, i.e. build materials are the intended tissue components (cells and hydrogels), whereas support materials create a negative sacrificial mold and hold the structure by giving mechanical strength. Support materials are either relatively deposited with build material or exists as a support bath. The sacrificial support material will usually be removed post processing. Shape fidelity (while the bath is removed) can be enhanced by incorporating crosslinker into the bath. Support hydrogel material is usually fabricated using reversible crosslinking mechanism.
5	Hybrid bioprinting	Bioprinting is integrated with other fabrication processes, for example, multiscale parts can be build by integrating inkjet or extrusion bioprinter with electrospinning or melt-plotting apparatus.

Injectability of the material is also important, since the injection parameters affect to the stability and resolution of the printed structure. Therefore materials intended for printing need to be characterized well using both quantitative and qualitative techniques. [15] In addition to injectability, printability and mechanical properties, characterization of the bioink's flow, degradation and swelling properties will give information about its performance and about the created 3D structure in physiological conditions [19].

This review article presents some design aspects and characterization of 3D-bioprintable hydrogels for extrusion-based bioprinting. In short, some bioprinting technique related design aspects, hydrogel property requirements for ideal bioink, and biological aspects of 3D-bioprinting of hydrogels are presented, followed by the characterization of pre- and post-printing properties of bioinks. Last, the challenges and future prospects of 3D-bioprinting are discussed.

2. 3D-bioprinting techniques and technique related design aspects

2.1. 3D-bioprinting techniques

Bioprinting techniques that are suitable for cell delivery are extrusion-based (EBB), droplet-based (DBB) and laser-assisted (LBB) bioprinting and stereolitography [20–23]. The focus of this article is on EBB, but also other techniques are shortly presented. Different bioprinting techniques are also compared in Table 2.

In EBB, based on the CAD design, the bioink's controlled extrusion (from syringe or nozzle) is done by using mechanical compression (pushing a piston or rotation of a screw) or pneumatic pressure in the form of cylindrical layer-by layer depositions [3,5,6,24,25]. The bioink is continuously extruded as a filament with size of approximately 150–300 μm in diameter on a receiving substrate [19,26]. Due to filament's continuous deposition, better structural integrity can be achieved, which also makes extrusion the most suitable for creating large-scale constructs [3]. The piston-driven system may give more direct control of bioink flow, whereas screw-based system can provide better spatial control and capability to dispense higher viscosity bioinks, although there are larger pressure drops harmful to suspended cells [3,6]. Pneumatic systems can also be used to print high-viscosity inks [6]. In general, suitable viscosity range for extrusion printers is from 30 mPa/s to $>6 \times 10^7$ mPa/s [6]. The cell viability is usually between 40% and 80%, but could be even 97% if printing parameters (e.g. temperature, pressure, deposition rate) are optimized [3,27]. In EBB, the cell viability may be affected more by the dispensing pressure than the nozzle diameter [6]. The EBB is simple and flexible, medium cost method capable to handle large amount of bioink and encapsulate high cell densities (also spheroids), and it can be used to create multi-material devices with multiple cell types and complex constructs [6,23–25,28]. The downsides are, however, relatively low printing speeds, relatively poor resolution (>100 μm) and potential nozzle clogging [3,22,24,29]. EBB can also cause cell damage and death, as well as cell aggregation and sedimentation due to shear stress and small nozzle's orifice diameter [28]. In general, EBB has the lowest survival of cells reported among the techniques [23].

Inkjet-based bioprinting, a type of DBB, is a noncontact printing method (between the nozzle and the substrate) that forms multilayered droplets and leads to small-scale 3D constructs [3,22,25,31]. From two function modes, continuous (CIJ) and drop-on-demand (DOD), DOD is the more commonly used with two different types, piezo and thermal inkjet printing, i.e. the actuator creates pulses leading to individual droplet (predefined ink volume) ejection through thermal or piezoelectric heads [1,20,25]. In thermal inkjet printing, despite the heating element's high temperature (300 °C), the cells are not affected by it due to short exposure time (2 μs) [26]. Droplets form if bioink's surface charges are weaker than surface tension. The material properties and droplet velocity (typically 5–10 m s^{-1}) will determine whether the drop

Table 2
Comparison of printing techniques suitable for bioprinting. Figures reprinted with permission from Jeong et al. (2020) [30] Copyright © 2020 MDBI.

Technique	Extrusion [3,6,19,22,24,26,29]	Inkjet [3,5,6,21–24,26,28,29]	Laser [3,22,24,26,29]	Stereolitography [22,23,29]
	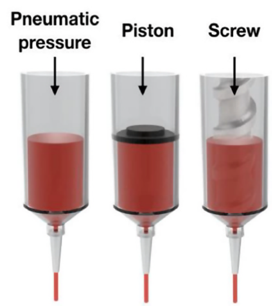	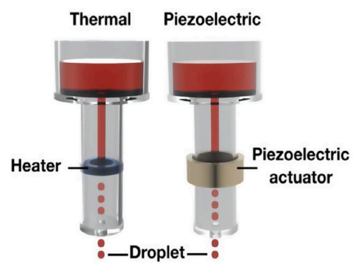	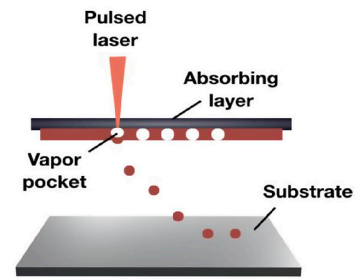	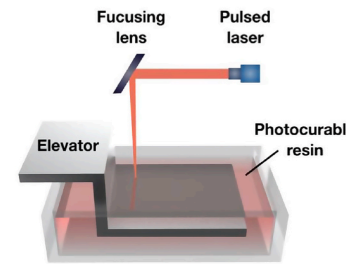
Filament/droplet*	Filament	Droplet	Droplet	Droplet
Size of *	150–300 μm diameter	10–50 μm diameter (1–100 pL)	20–80 μm diameter	50–100 μm diameter
Resolution	Medium	High	High	High
Viscosity range	30 mPa/s to >6 × 10^7 mPa/s	3.5–12 mPa/s	1–300 mPa/s	100-10 000 mPa/s (no limits)
Printing speed	Slow	Fast (up to 10 000 drops/s)	Medium	Fast
Cell density	High (~10^8 cells mL^{-1})	Low (10^6 cells mL^{-1})	Medium-high (~10^8 cells mL^{-1})	Medium
Cell viability	40%–80%	>85%	>95%	>90%
Cost	Medium	Low	High	Low

will keep its shape or splash [31]. Small droplet size may lead to weak mechanical properties of printed tissue and increased processing time [22]. DBB is a simple method, with possibility of rapid deposition using multiple nozzles allowing simultaneous printing of multiple material and cell types [3,5,6,21–24,28,29]. High accuracy and resolution constructs can be printed, since the deposition rate and droplet size are highly controllable [32]. However, even though DBB can provide accurate positioning of cells and high resolution, bioink should have low concentration and relatively low viscosity to enable the formation of a droplet leading to inefficient encapsulation of cells and poor structural integrity (at the droplets' interfaces), as well as low cell concentration/density [22–24,29]. Downsides are also the risk to expose materials and cells to mechanical and thermal stress, nonuniform droplet size, low droplet directionality and possible clogging of the orifice [3,6,21,28]. With piezo inkjet printing, uniform droplet size and ejection directionality can be controlled, but also pressure and heat stressors are avoided [6]. Compared with EBB, there are less useable bioink types in DBB, as well as no ability to print a filament under continuous flow, or more complex constructs with clinically relevant sizes [3,5,29]. Also, there are no readily available inkjet bioprinters [2]. The frequencies (15–25 kHz) used also leave some concerns relating to possible cell damage [6].

In LBB, a focused laser beam illuminates a ribbon carrying a bioink layer at the bottom and photoabsorbing layer on top side [3,24,26]. The positions where the laser hits endures localized heating leading to formation of bubbles and propelling the bioink droplets towards the stage moving along z-axis [24]. To fabricate the final construct, the process will be repeated in a layer-wise fashion several times [3]. The cost of LBB is, however, higher than with other methods [24,26]. Since LBB is a nozzle-free method, there is no clogging or shear stress problem [20,26]. LBB is also a very complex process compared with EBB (and DBB), for example relating to the use of laser which affects to viability of cells (long-term effects are also unknown) and material properties (more limitations for materials than with DBB) [3]. LBB has also a limited scalability (used to form small scale constructs) and low stability [21,23,25]. On the other hand, LBB has the highest precision and resolution compared with EBB (and DBB) [3,29]. It is also possible to print multiple materials and cell types with LBB [3]. Rapid gelation kinetics is required for high resolution in order to achieve high shape fidelity [28]. Factors, such as the bioink layer's viscosity and thickness, the air gap between the collector platform and donor substrate, or the laser parameters will affect to LBB [26]. LBB has two types, photopolymerization (i.e., stereolithography) and cell transfer (i.e., laser-induced forward transfer) [3].

Stereolithography (SLA) is a nozzle-free system that uses light for the polymerization of light-sensitive inks in a layer-by-layer deposition [2,22,29]. The printhead moves in only one direction [22]. SLA is a low cost method that uses short printing time (<1 h) and results high resolution [22,29]. Large viscosity inks can be printed [29]. High cell viabilities can be achieved despite the possible cell damaging effect of UV light used in photocuring [22,29]. SLA lacks the affect of shear stress and does not have viscosity limitations for bioinks [23]. The limited choice of photosensitive biomaterials however limits its use [23].

2.2. Bioprinting technique related design considerations

Selection of suitable printing technique is important, since it affects, for example, to the selection of bioink and their printability as well as to the properties of the printed construct. In general, requirements for the printer are user friendliness, affordability, full automation capability, easy of sterilization, sufficient build speed, compactness and versatility [22]. More precisely, if considerable mechanical strength is needed, extrusion based printing is usually used. This can be done by using so called support materials i.e. extruding the gel into a secondary support gel. [3] Mechanical properties can also be enhanced by using secondary light- or UV-induced crosslinking after extrusion [3,33]. However, the possible cytotoxicity of photoinitiators and the damaging effect of UV-irradiation should be considered in the case of UV-crosslinking [14,23]. By using visible light instead, these risks can be overcome and the light can actually penetrate to a greater depth. Better shape fidelity and cell compatibility can also be achieved. [33–35] Also, the viscosity and surface tension of bioink should be considered, i.e. low viscosity materials are suitable for jetting techniques, whereas with EBB using high viscous material the gelation mechanism and viscosity will be limiting factors [6,9,26]. EBB also requires shear-thinning properties, since withstanding of high shear forces and rapid recovery (self-healing) after are needed for protection and better viability of cells [6,19,26].

Bioprinting speed, biofabrication time, nozzle diameter, extrusion pressure and dispensing speed are the major bioprinting parameters, that should be optimized in order to get optimal outputs such as diameter, precise placement, uniformity or filaments' spacing distance during the printing and encapsulated cells' viability post-printing [1]. The feeding rate, printing speed and pressure and the distance between the printer substrate and nozzle need to match [36]. Nozzle diameter determines the required deposition time of material to form the 3D structure. For example, DBB requires fast crosslinking time, whereas with EBB final crosslinking happens after fabrication since viscous materials can maintain the 3D shape after deposition. [6,26] However, since nozzle diameter is directly related to resolution, it might restrict the viscosity of material and affect to shear stress [26]. Further, the smallest material unit formed and layer thickness will determine the printed construct's accuracy and resolution. For example, in DBB the smallest unit is droplet, whereas in EBB they are strands and droplets. In stereolitography, the spot size or beam area of laser will determine the cured photopolymer's resolution. Different resolutions have been collected by Lee et al. [9]. In terms of layer thickness, other printing parameters such as nozzle diameters, path space and path height can affect to it. [9] Biofabrication time, on the other hand, is the time embedded cells are exposed to bioprinting i.e. cell viability will be reduced if the printing time is too long [1]. Sterilization can also be considered as a parameter that affects to construct's resolution, structural integrity and anisotropy. Tissue scaffold's sterilization can be done either before the printing leading to sterile scaffolds or following the formation of scaffold using traditional sterilization methods. [37]

In biological point of view, the printing system needs to be suitable for the cells that need to survive the process. With nozzle-based techniques (DBB and EBB) the varying size of different cell types (single cells 10–30 μm, cell spheroids 150–500 μm) determines the size of the nozzle. [9,22] In DBB, bioink's material components can alter the droplet integrity. The droplet splashes or spreads if the integrity is lost and therefore the structure may fail or cells may be deposited from their position. [22] For DBB the critical feature is the fluid mechanics. The surface tension is inversely proportional to the bioink's cell concentration as more cells can be absorbed to the liquid-gas interface. Also, low cell densities ($<10^6$ cells mL^{-1}) are needed for DBB. [3] For efficient exchange of nutrients and oxygen, optimal pore size would be about 100 μm, however, for example, for EBB it is problematic to extrude cell-laden hydrogel through such size of a fine nozzle [5]. The bioprinter should enable the printing of different cell types together with biomaterials and result high resolution structure (depends on the accuracy of printer) [22]. Also, material choice influences to material's ability to protect cells during the process, for example, thermal inkjet printing contains localized heating of material affecting to cells that can be prevented by using materials with low thermal conductivity or "cushioning" ability [6]. In terms of stem cell differentiation triggered by shear and mechanical stress, DBB could be considered much gentler process compared with EBB. However, EBB could be modified by optimizing the back pressure or by including shear thinning materials. Also, when using EBB (or DBB), stem cell multipotency can be retained by using hydrogel bioink that have limited cellular interaction. [20] Because stem cells are sensitive to external stimuli, the bioprinting process should not trigger them in unwanted manner. With this in mind, the printing process can be either neutral or stimulatory. In neutral, the differentiation of stem cells is triggered by the culture conditions, whereas in stimulatory approach the properties of substrate and environment can stimulate. [20]

Panwar et al. [38] have nicely collected a figure (Fig. 1) showing the relationship between bioink consistency, printing parameters and cell laden bioink. Printing conditions include: printing speed, dispensing pressure, nozzle diameter and temperature and chamber temperature. Bioink consistency includes: viscosity, viscoleastic properties, hydrophilicity, shear-thinning properties, molecular weight, type and extent of crosslinking, and gelation point. The optimization of these parameters will lead to better resolution and cell viability. Cell viability will be affected by the nozzle diameter, dispensing pressure and bioink consistency since they determine the shear force experienced by the encapsulated cells (Fig. 2 (a) and (b)). For example, with increased nozzle diameter, cell viability is increased as shear stress will be decreased, but the resolution gets compromised. [38] This is important, since if short-term high level shear stress is experienced during the printing it has been shown to affect to cell viability but also there might be some long-term alterations in proliferation as well as in the functionality of survived cells. In fact there may exist a threshold of shear stress for certain cell types. [10] The printing parameters should also be chosen according to particular cell type and bioink composition. Further, the development of bioink based on different cell types is needed. Bioink's concentration also affects to cell viability, i.e. as concentration increases the viability decreases as cell migration and diffusion are prevented due to entangled network. [38] Further, by optimizing parameters, like cell concentration, time of printing, temperature (reduced temperature preferred) and oxygen diffusion, problems such as diffusion-limited cell seeding or cell gradients can be avoided [37].

3. Design aspects of bioink and tissue construct

3.1. Ideal bioink

Bioink, by definition from Groll et al. [39], is "a formulation of cells suitable for processing by an automated biofabrication technology that may also contain biologically active components and biomaterials". Hydrogels are the most outstanding biomaterials, whereas biologically active components can be, for example, adhesive peptides, growth factors, DNA etc. Cells can be, for example, human, animal or plant based cells, alone or as a combination. [1,38] There are five types of biomaterial bioinks (i.e. hydrogel-based biomaterial & encapsulated cells) that can give characteristic properties (Table 3) [1]: single component hydrogel, supramolecular hydrogels, interpenetrating polymer network (IPN) hydrogels, nanocomposite hydrogels, and multimaterial inks.

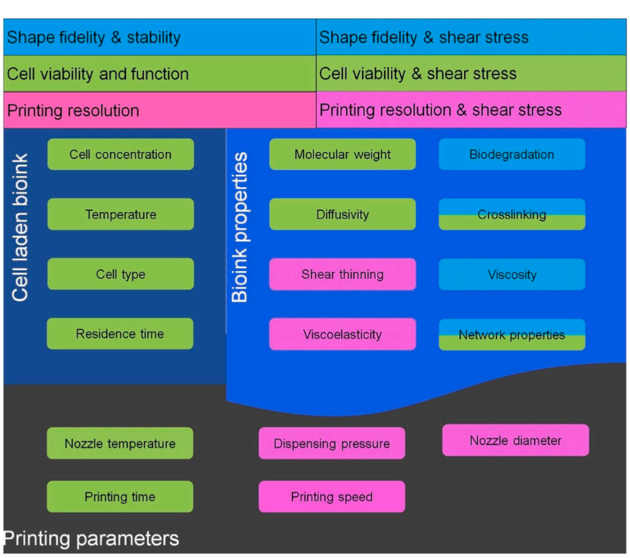

Fig. 1. Relationship between printing parameters, bioink properties and cell laden bioink. Reprinted with permission from Panwar et al. (2016) [38] Copyright © 2016 MDBI.

Despite similarities to injectable hydrogels, the requirements for ideal 3D-(bio)printable hydrogel inks are more strict. Ideal bioink should be extrudable, printable and easily manipulated by the printer, have controllable chemical, physical, functional, material and biological properties, have suitable viscosity and rheological properties, contain sterile and endotoxin free starting materials, be stable during printing procedure, enable homogeneous distribution of cells, and consider manufacture impact on cell viability (i.e. chemical cytotoxicity, pressure-induced apoptotic effect etc.). [1,3,6,22,23,29,31,40–42]

So called biofabrication window can be used when designing bioinks. It is a multiple parameter analysis that visualizes parameter interplay. [43] For example, Fig. 3 shows how the printability of bioink (i.e. suitability for fabrication) can be optimized while maintaining the cellular activity [11,19,44,45]. Traditionally more crosslinked, stiff materials result high shape fidelity, but have reduced biological performance (e.g. cell differentiation, proliferation etc.). More novel and advanced approaches can expand the biofabrication window and enable printing of lower stiffness materials, yet resulting high shape fidelity. [43]

3.2. Ideal 3D-bioprinted tissue construct and biological aspects of bioprinting

There are different requirements for ideal 3D-bioprinted tissue construct: it should mimic the aimed tissue as much as possible, have quick (re)gelation after printing (ensures shape stability), have self-supporting structure (no post-processing stabilization needed), have structure that tolerates dynamic mechanical load and biochemical & mechanical stimulation and shape & size flexibility, have minor or no swelling, and have structure that promotes nutrient and metabolic waste product transportation, support (fast) vascularization, and promote cell (in)growth and proliferation and cell signaling [1,3,6,22,23,29,31,40–42]. Different biological aspects are especially important. Next, some functionalities of native-like bioprinted tissue that should be addressed are shortly discussed.

3.2.1. Cell source

The most commonly used cell sources in bioprinting are the terminally differentiated cells due to large quantities, wide availability, well-characterized functionalities and ease of maintenance [24]. In general, for bioprinting the cell sources should be nonimmunogenic, easily expandable in culture, readily available and able to reproduce tissue functions [6]. The choice of cell type should be done according to their mimicry of *in vivo* physiological state of cells and how they maintain their functions [6,46]. Also, an expanding into sufficient number of cells for printing is needed. The *in vitro* and *in vivo* cell proliferation control is needed, i.e. too little results in loss of viability, and too much in apoptosis or hyperpasia. [6] For example, pluripotent stem cells have shown a great potential due to ability to generate large number of cells [6,47]. Other suitable cell types are mesenchymal stromal cells (MSCs), and adult stem cells from fat, bone marrow etc. [48,49]. The cells should survive the printing process and once transplanted they should withstand physiological stresses (e.g. shear stress, pressure, biological stressors) [6]. In ideal case, the stem cells would be from the patient causing no undesirable local or systemic responses [3].

3.2.2. Cell density

Native organs consist of multiple cell types in varying, often high, densities. In order to replicate that in bioprinting, the bioink and bio-

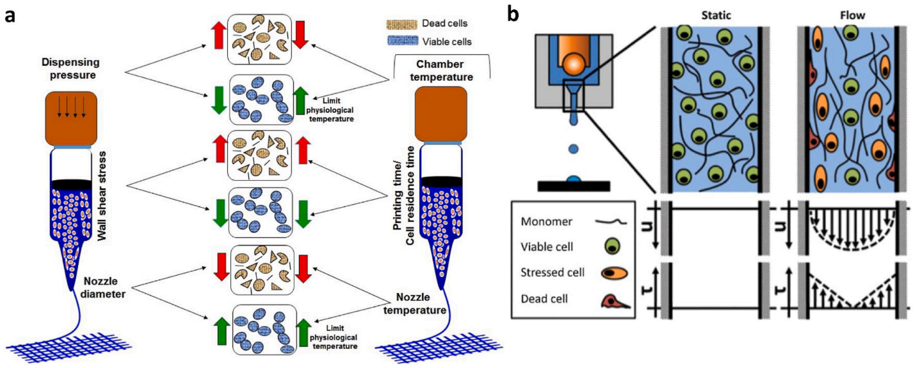

Fig. 2. (a) Effect of dispensing pressure, chamber temperature, nozzle diameter and temperature, printing time, and wall shear stress on viability of cells [38], and (b) distribution of cell-laden hydrogels' shear stress (τ) and velocity (u) inside a nozzle [5]. Reprinted with permission from Panwar et al. (2016) [38] Copyright © 2016 MDBI and Li et al. (2018) [5] Copyright © 2018 Elsevier.

printing modality should be considered. [3] High density of cells (0.1 billion cells/mL) without affecting to viability can be achieved by using EBB (viscous bioinks), whereas DBB gives lowest density ($<10^6$ cells/mL) and viscosity [50,51]. In general, in scaffold-based bioprinting the density is less than 10^7 cells/mL [3]. Cell density influences to the behavior of cells and ECM production, and thus also to the structure and function of bioprinted construct. Too low cell density can result insufficient cell-cell interactions and thus construct may not support the tissue growth, whereas too high cell density can lead to overcrowding of cells leading to cell death or insufficient nutrient supply, and finally to tissue necrosis. [52] All in all, better cell-cell interactions and faster formation of tissue can be achieved with higher cell content, but the viscosity and printability of bioink may be affected [3,26]. For example, there are results showing that as cell density increases also the viscosity of bioink increases, but there are also opposite results showing that viscosity, as well as G', gelation kinetics and yield stress may decrease [27,53–57]. There are also examples about how mechanical, structural or functional properties of bioprinted constructs, as well as post-bioprinting cell differentiation, proliferation and interaction are affected by the cell density [58–62]. ECM remodeling has also been shown to be accelerated by the higher cell seeding density [63]. Since cell groups are located in various locations in organs, the high cell density's spatial placement is important [64]. The printer resolution affects to the spatial placement, for example EBB has lowest resolution (>100 μm), DBB in the middle (50–100 μm) and LBB the highest (20 μm) [3]. The spatiotemporal location and final density of cells are affected by the initial cell density, gelation concentration, temperature and elapsed time from initial cell suspension [64]. The cells would be kept in initial place better in more solid bioink [3].

3.2.3. Heterogeneous cellular structures

Most organs have complex heterogeneous nature [3]. The engineered tissue's performance can be improved by using heterogenous cell population (co-culture system) [9]. Currently some bioprinters are able to print heterogeneous cellular structures as they can deposit more cell types at once. However, DBB is more suitable for this than EBB (or LBB), because the multiple cell types can be bioprinted as a droplet (<100 μm). [3,65–67] Bioinks can be made heterogeneous mixtures too, for example by combining the soft hydrogel component with firm substances, like nano-fibrillated cellulose [68], hydroxyapatite [69], dual-crosslinking [70] etc. for better mechanical properties. Other properties, such as thermal and electrical properties (adding graphene [71]), enhanced bone formation (adding bioactive glass [72]), ECM elements (given by self-assembling peptides [73]), or bioelectric properties enhancing cardiac cell function (adding gold nanorods [74]) can be achieved too. Chemical (e.g. growth factors [75], cytokines [76] etc.) and physical (e.g. stiffness [77], porosity [78], fiber alignment [79] etc.) gradients, present in native cellular microenvironment [80], can also be added in order to induce certain cellular response. Multi-material deposition can be enabled by the bioprinting modular setup with increased number of printheads [9]. One example about bioprinting heterogeneous gradients is aortic valve, i.e. how to control the material placement so that complex, hierarchical structures with spatially varying feature sizes and properties of aortic valve can be achieved so that coronary flow, tissue dynamics and efficient blood flow dynamics function properly [81–84]. Multimaterial bioprinting is needed due to anisotropy in the structural and mechanical requirements as well as cell type distribution heterogeneity of native valve [85].

3.2.4. Mimicking of functional accuracy

Biomimicry, more specifically functional accuracy (e.g. complex neural structures, internal vasculature and circulation), of printed tissue is desired in bioprinting [3]. The cell shape and size will be determined by the biomaterial used and surrounding environment. For example, by using natural polymers, similar to native ECM, as single or multicomponent bioinks, biocompatible, biodegradable and cell growth and function supportive structures can be created [86]. Added surface ligands give also biomimicry by improving the attachment and proliferation of cells on the material substrate. Attachment (and differentiation) of cells can also be improved by using nanoscale surface features such as notches, ridges, grooves and steps. [3,6,20,87] The construct's 3D-environment also affects to differentiation process and cell shape [6]. In order to reproduct tissue's cellular and extracellular components, the vascular tree branching patterns can be mimicked like will be shown in the next chapter, or previously presented physiologically accurate gradients and types can be manufactured, all in microscale. Therefore microenvironment is important to understand. [6] One example emphasizing the need of biomimicry is how to mimic the structure of kidney's glomerular basement membrane (GBM) that has different chemical, surface and mechanical properties that enable filtering the blood i.e. molecular sieving and water retention which a dialysis machine cannot do efficiently [88,89]. Bioprinting functioning kidney structures is still a relatively new area of study and a multimaterial bioprinting or a combination of printing techniques may be needed to build these complex structures [90,91]. Bioprinting has also been used together with on-a-chip systems to fabricate and study glomerulus models for disease modelling or drug screening, although glomerular modelling with this method is still to be fully assessed [92,93]. However, even if the construct would contain same materials and have similar structure to native organs, some properties might still be different due to distinct functions of complex organs, such as hormonal and protein secretion, filtration, and protection. This should also be considered when designing the construct. [3] Thus, the understanding of the complex structures and functions of natural tissues and organs would help to design better biomimetic 3D-bioprintable constructs.

Table 3
Biomaterial bioink types [1].

#	Type	Components	Properties
1	Single component hydrogel	Single component hydrogel + encapsulated cells	The printability may be approved by increasing the polymer concentration and crosslinking density, although it may harm the cells as porosity will be decreased.
2	Supramolecular hydrogels	Supramolecular hydrogel + encapsulated cells	Printability and productivity can be improved, and they also offer tailorable surface structures for cell-scaffold interactions, favourable mechanical properties (high mechanical strength) and biocompatibility, modular bioprinting and Lego-like assembling (two direction printing i.e. direct printing of gradient constructs, or printing different constructs that self-assemble into complex structures) with controlled chemical, physical and cellular components at higher resolutions.
3	Interpenetrating polymer network (IPN) hydrogels	Hydrogels (physically interweaved networks with each other) + encapsulated cells	The printability can be improved using both physical and chemical crosslinking, and the construct will have improved fracture strength and toughness.
4	Nanocomposite hydrogels	Engineered nano-composite hydrogel (hydrogel & nanoparticles) + encapsulated cells	Depending on the type of nanoparticles the physical, biological and chemical properties can be dramatically different, and functionality, printability, usability and degradability can be regulated.
5	Multimaterial inks	Multiple ink materials (at least one is hydrogel) + (multiple) encapsulated cells	The hydrogels are crosslinked together, and can create complex gradient constructs with desired functionalities, morphology, structure, mechanical characteristics etc. and defined geometries. Also, the location specificity of cells and combination of multiple cell types are enabled.

3.2.5. *Vascularization*

Complex vasculatures of organs *in vivo* provide a blood flow in order to sustain the functionalities and necessary supplies. Thus, vessel-like structures are also needed for engineered constructs, i.e. constructs with over 200 μm thickness need vascularization in order to transport nutrients, oxygen and waste [3,10]. Latest bioprinting techniques enable the printing of vasculature at the same time with other components leading to complex vascularized structures. The problem is however the resulting heterogeneity in construct. [3] One aspect that should be noted is the need for different approaches for micro- and macro-vascularization, since in nature they have different structural function and composition [94]. Submillimeter-sized capillaries consist of a single endothelial layer that enables permeability, whereas larger arteries and their smaller branches (arterioles) have a layered wall structure via which blood transports to capillary bed (gas and nutrient exchange). [94] Macrovessels have been able to biofabricate *in vitro* although with limited mechanical integrity [95,96], whereas microvasculature is still a challenge. The bioprinting of small capillaries *in vitro* is difficult because many technique is able to make only >100 μm diameter vessels [3]. Therefore, bioinks may need added cues promoting vessel formation. This kind of microvascular network self-assembling can happen either by angiogenesis (forming of capillary networks starting from a pre-existing vessel, e.g. capillary sprouting [97]) or vasculogenesis (new formation of vascular structure/primitive vessel network, typically in embryonic development). [94,98]

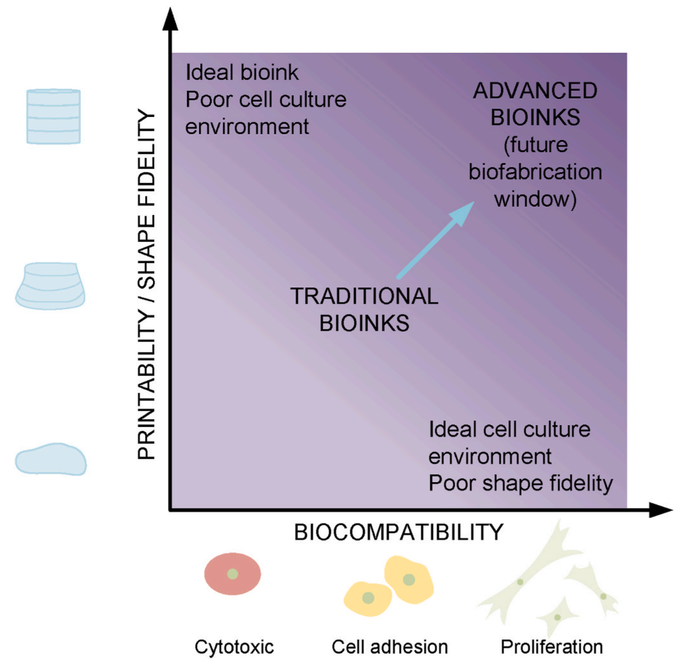

Fig. 3. Biofabrication window. Figure inspired by Malda et al. (2013) [44] and Chimene et al. (2016) [45].

Vasculature has been bioprinted in two ways. EBB has been used to print channels by using fugitive inks and endothelialization. [3] This sacrificial bioprinting used for the formation of hollow vessels consists of four steps: (1) solid sacrificial microfibrous bioink is deposited, (2) hydrogel embedded with stromal cells are cast over the templating micro-fibers, (3) perfusable channels are formed by selectively removing the fibers (e.g. temperature-induced phase change, dissolution or mechanical extraction etc.) under conditions suitable for the cells, and (4) functional vessels are build by seeding the endothelial cells in the interiors of the microchannels. This method is considered as indirect bioprinting. [10,24] In alternative way the channels are printed using direct bioprinting [3]. Bioprinting strategies to fabricate vascularization can further be divided in four groups [94]: 1) sacrificial bioprinting [99], 2) sacrificial writing (e.g. sacrificial writing into functional tissue, SWIFT [100]), 3) submerged bioprinting (e.g. freeform reversible embedding of susbended hydrogels, FRESH [101]), and 4) coaxial bioprinting [102].

Since various cell sources can be used for vascularization, most recent studies have used multiple cell lines for vascular tissue formation. For example, De Moor et al. [103] combined ECs with fibroblasts and adipose tissue-derived mesenchymal stem cells (ASCs) as supporting cells to generate prevascularized spheroids. By combining them with a photo-crosslinkable methacrylamide-modified gelatin (GelMA) and Irgacure 2959, they were able to bioprint small diameter capillary-like microvessels. This study showed the potential of triculture prevascularized spheroids as multicellular building blocks. [103] Liu et al. [104], on the other hand, bioprinted soft hepatic tissue at centimeter scale with branched perfusable vascular networks with proper vascularization and hepatocytic function *in vitro*. They used multi-material bioprinting with cell-laden inks (GelMA-fibrin, HUVECs, MSCs, HepG2 cells), fugitive inks (10% gelatin-based), and elastic inks (10% GelMA or PDMS). Since biofabrication of living tissues/organs depends on the integration of vascular networks *in vivo*, Liu et al. also fabricated an inner and external pressure-bearing layer in their structure so that multiscale vascular network can survive under physiological blood flow. This was the first time a bioprinted multiscale perfusable vascular tree within 3D hydrogel was bioprinted. [104] More recently, Liu et al. [105] fabricated centimeter-scale 3D-bioprinted cardiac patches with well-organized and high-density microvasculature by bioprinting spheroids of early vascular cells (EVCs) and cardiomyocytes in ECM hydrogel. Self-assembly vascularization of EVC spheroid showed to be superior to EVC single cells. [105] Same year, Shen et al. [106] fabricated vascularized tissue-engineered bone with biological activity. Large bone defects are challenging since newly formed bone tissue lacks effective vascularization. Thus, they bioprinted vascular endothelial cells with thermosensitive bio-ink *in situ* on the inner surfaces of bone mesenchymal stem cell-laden bioprinted scaffolds' interconnected tubular channels. A more uniform distribution and greater seeding efficiency throughout the channels was exhibited by the endothelial cells, which promoted tube formation and vascular network formation through culture. *In vitro*, these vascularized scaffolds also had a coupling effect between osteogenesis and angiogenesis. *In vivo*, in rat calvarial critical-sized defect models new bone formation was also promoted. [106]

There are different properties and composition of bioink that can influence to vascularization, for example Salg et al. [94] have collected a table showing how bioink's physical properties and construct geometry (i.e. porosity/interconnectivity, pore size, architecture), biochemical properties (i.e. ECM composition and structural binding motifs in bioinks, proangiogenic signaling molecules, oxygen-producing bioinks, hydrogel concentration), and cellular composition (i.e. ECs, HUVECs, Human induced pluripotent stem cells (hiPSCs), Pericytes, smooth muscle cells and fibroblasts, Mesenchymal stem cells (MSCs)) affect to vascularization.

3.2.6. Innervation

A process by which nerves grow and form connections with target tissues or organs is called innervation. Innervation promotes the development of tissues and organs, but also has a central role as a tool for their functional control and modulation [107]. Innervation is needed, for example, for the function of cardiac, skeletal or smooth muscle containing tissues (e.g. stomach or bladder) [32,107]. Since innervation is also needed in tissue engineering for the proper functioning and integration of the implanted constructs with the host tissue, bioprinted constructs should also have channels for nerve innervation [32]. Conduits should be biodegradable since non-degradable can lead to inflammation [108]. In order to achieve innervation into the construct, growth factors (e.g. neurotrophic factor [109]), electrical stimulation [110], physical guidance cues (e.g. microchannels [111]), and co-culture with nerve cells [111] have been used. It should also be noted, that since many times nerves and blood vessels follow the same paths, they are considered functionally coupled, for example, promoting innervation can promote angiogenesis due to neuropeptides released by autonomic and sensory nerves [107,112]. For example, Kim et al. [111] investigated the effects of neural cell integration (by human neural stem cells (hNSCs) and human muscle progenitor cells (hMPCs)) into the bioprinted skeletal muscle construct (cell-laden fibrinogen-gelatin-hyaluronic acid (HA) bioink, sacrificing acellular gelatin-HA bioink, and supporting polycaprolactone (PCL) bioink) to improve the functional and structural recovery of muscle defect injuries. Microchannels were created by removing the bioprinted sacrificial patterns. An improved myofiber formation, long-term survival, and neuro-muscular junction formation *in vitro* were achieved. Also, this neural cell integration facilitated rapid innervation and construct matured into organized muscle tissue, proven by a rodent model. The bioprinted muscle constructs were also highly vascularized following implantation into the muscle defects. [111] Next year, Ngan et al. [113] created matured myofibers in bioprinted constructs with both *in vivo* innervation and vascularization. They delivered primary mouse myoblasts in a single material bioink (gelatin methacryloyl (GelMA)), and implanted that into *in vivo* chamber in a nude rat model. For the first time, myoblast migration through the bioprinted GelMA, leading to spontaneously forming fibers on the surface, was demonstrated. Thus, without material hindrance, an advanced maturation and the connection between incoming nerve axons and vessels *in vivo* were enabled. [113]

3.2.7. Mechanical properties

Suitable rigidness is needed for structure maintenance, whereas suitable porosity is needed for cell growth and vasculature. For example, the rigidity of soft native tissues (e.g. brain) is around 0.2–5 kPa, whereas with hard tissues (e.g. bone) up to 15,000 kPa [114]. Differentiation of neuronal and adipose tissue is promoted by soft elastic scaffolds (0.1–5 kPa), whereas bone, cartilage and muscle differentiation is promoted by firmer scaffolds (8–30 kPa) [115,116]. Construct's mechanical properties will be affected by the bioink's crosslinking speed and strength, viscosity and yield stress, and will vary according to temperature and time. Suitable bioink's malleability is needed for printing, but at the same time the shape should be retained post-printing in order to get sufficient dimensional integrity and mechanical strength. Depending on sample's porosity, hardening will happen gradually with changing strength. [3] This should be considered especially in load-bearing tissues, for example, suitable layer thickness and printing orientation have shown to be important for achieving desired properties [117]. In addition, the cells affect to construct's mechanical properties, i.e. softer hydrogel constructs can be achieved with cell clusters (randomly distributed) compared with homogeneously distributed cells [26]. Also, hydrogel remodeling has been shown to be accelerated by the higher cell seeding density, which also can give higher construct's modulus. Dynamic loading conditions can also result higher modulus. [26] Mechanical stimulation (e.g. stretching) of construct can also be used before transplantation, for example for post-printing maturation of cardiac cells [118].

4. Pre- and post-printing properties of bioinks, and their characterization

Since the printed construct should mimic the cellular architecture and shape, printability is very important concept in bioprinting [11], in fact the most important parameter. Despite the widespread use of the term "printability", there lacks a consensus on when you can call material "printable". For example in case of EBB, printability can be referred to suitable extrudability, filament formation and shape fidelity (Fig. 4). [43] Printability usually involves viscosity, surface tension and crosslinking properties (e.g. crosslinking type, gelation kinetics) [2,8,19]. In rheological point of view, viscosity, shear-thinning and yield stress are important parameters [1]. For example in case of EBB, it is important to understand the ink's rheological properties in all of the three stages i.e. (1) extrusion stage (viscosity, shear-thinning, yield stress), (2) recovery stage (shear recovery), and (3) self-supporting stage (yield stress), in order to understand the printability and 3D structure evolution [25]. In addition to previous attributes, also biodegradation and biocompatibility, are affecting to printability [19].

Characterization of printability can be divided in two sections: pre-printing and post-printing. When printing is done with nozzle-based system, from a rheological point of view, printing is the flow of material through a contraction followed by tube flow. After ejection and

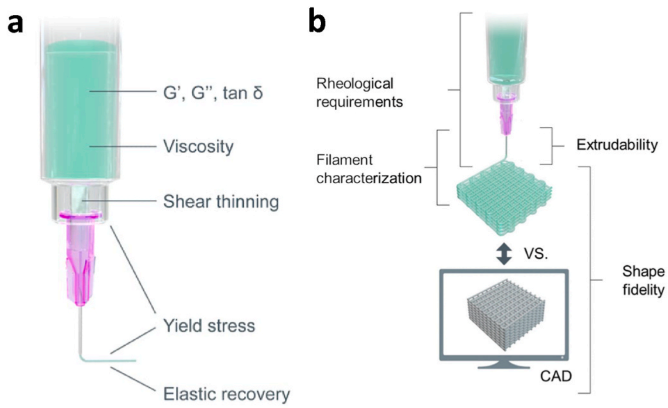

Fig. 4. (a) Rheological properties that affect to printability and shape fidelity, and (b) how to assess printability in EBB. Reprinted with permission from Schwab et al. (2020) [43] Copyright © 2020 ACS Publications.

deposition onto the collector, the material should undergo fast phase transition so that shape would be preserved and 3D structure fabricated. The process rate is crucial for successful printing, which as a demand is also a big difference between injectable and printable hydrogels. [31] During the printing process, shape fidelity, printability and cell viability are determined by the rheological properties. Bioink's post-crosslinking, on the other hand, determines their physiological stability, mechanical integrity, and cell functions and survival. [19] For the end application, the matured bioprinted construct's final properties are crucial. The amount of cells in the construct, proliferation, migration and integration with the material influence to these properties during the tissue formation. The mechanical requirements of printing process should be met, but at the same time cell survival within the construct should be ensured. [26] Many studies focus on the hydrogel construct's performance and properties after implantation, but for successful bioprinting of bioinks, their pre-printing properties and behavior are also critical and important to know [119]. Only few papers characterize the precursor solution, as they usually only state that the precursor solution of hydrogel is injectable based on ability to pass through a syringe needle. Gel formation has also been reported only based on a tube tilt test. [119]

The pre-printing characterization can be divided into: viscosity, yield stress, shear performance (shear-thinning property), recovery time (self-healing ability) and shape fidelity. Post-printing characterization of 3D-bioprinted construct, on the other hand, can contain optical image analysis (quality, spreading and printability of bioinks post-crosslinking), compressive mechanical analysis (mechanical stability and compressive modulus of construct), as well as swelling and degradation analysis (bioink's swelling ratio and degradation characteristics). Further, characterization of the effect of printing process on cell viability and evaluation of cell-material interactions should also be studied. Quantitative analysis of post-printing structures has shown to be difficult. Printability could also be semi-quantified using mathematical models or quantified using computational analysis. [11]

4.1. Viscosity

Viscosity tells how much the fluid resists the flow under a stress [5]. In case of 3D-printing, viscosity describes bioink's ability to flow through a reservoir and nozzle onto the printing surface [19]. Viscosity, together with nozzle diameter and printing pressure, can influence to shear stress, which further affects to cell biology [11]. High viscosity solutions as less flowable can ensure that bioink does not spread or droop on the printing surface, and the large structures do not collapse and can hold the shape longer post-printing, but on the other hand, need higher pressure for flowing (increased shear stress) which can be harmful to cells and make the handling and extrusion more difficult and fracture the printing filaments, therefore limiting the smallest print size [2,18,19,26]. High viscosity hydrogel inks also have reduced porosity which may prevent cell spreading and migration [5]. The sedimentation of cells caused by unsuitable viscosity leading possible nozzle clogging or inhomogeneous distribution of cells through the construct should be avoided [31]. Since sufficient viscosity is required to maintain the construct's shape, but high concentrations restrict cell proliferation, it would be most logical to use hydrogels with low concentration and high viscosity for printing [5].

Viscosity depends on the molecular weight and concentration of the polymer solution, degree of branching and addition of rheological modifiers, as well as temperature [1,19,26]. Across all shear rates, increased viscosity will result from increase of those parameters (except temperature) [19]. Viscosity affects to efficiency of cell encapsulation (e.g. allows cell encapsulation uniformly), but also shape fidelity [1,2,23]. If surface tension between the bioink and nozzle diameter is increased, the bioink's ability to shear thin will decrease. Whether the extruded material is a droplet, continuous filament or a strand depends on the viscosity of bioink, i.e. filaments are formed with higher viscosity, whereas low viscosity leads to strands spreading out to receiving platform. [19,26] Tirella et al. [120] have nicely developed a 3D phase diagram (processing window) that illustrates the interrelationship of applied pressure, print velocity and bioink's viscosity [120].

Tunable viscosity of bioink is preferred in order to be compatible with various printers, i.e. the viscosity is around 10 mPa s for DBB printers, 6 to 30 $\times$ 10^7 mPa s for EBB printers and 1–300 mPa s for laser-assisted printers [2,42]. If higher viscosity solutions are used for DBB and EBB, shear-thinning materials should be used for the compensation of high shear stress [2].

Viscosity is usually studied in the literature together with printability and rheological studies [11]. Oscillatory amplitude or frequency sweep are used to determine the storage modulus (G') and loss modulus (G'') from pre-crosslinked or post-crosslinked bioinks, whereas a rotational shear rate sweep is used for viscosity (η) determination [19].

4.2. Shear-thinning properties

Shear-thinning materials are non-Newtonian fluids that have shear-rate-dependent behavior, i.e. the viscosity decreases when shear rate increases [26,31,121]. Shear-thinning is important for printability, extrudability and injectability [1]. This is because bioink's deposition is facilitated when viscosity decreases due to applied pressure in the nozzle, leading to high shape fidelity [26]. When hydrogel is extruded it undergoes shear i.e. physical crosslinks are broken and chains are aligned, which reduces the viscosity as extend of entanglements is decreasing [5]. The decrease of proportional shear force enables extrusion even through a small nozzle sizes [119]. The bioink's viscosity increases again as the shear stress is removed. This is also why this phenomena is useful for nozzle-based systems. [26] If material does not shear thin, it may clog the nozzle [119].

For 3D-bioprinting, the material's shear performance through the tube, nozzle or needle is important [119]. Shear-thinning self-healing hydrogels would be great materials for 3D-(bio)printing to overcome many challenges of it. For example, the printing speeds could be increased without construct property deterioration, and the interlayer adhesions between weld lines could be improved. Probably the production of more complex constructs would also be possible by using these dynamic inks. [29] Also, shear-thinning hydrogels could possess cytoprotectiveness during the injection due to shear banding and plug-flow velocity profiles limiting cellular membrane's disruption during shear flow, without the need to compromise in terms of shape fidelity or printability [19,40]. Cells can also spread more within the dynamic network compared with static counterpart [29]. Additionally, there is a pressure drop as the bioink goes from syringe to nozzle whose effect can be normalized by using shear-thinning bioinks as bioinks chains slide at the junction. Also the resolution is enhanced as shear-thinning bioink smoothly flows through the nozzle. [38] After printing highly shear-thinning hydrogel would provide sufficient mechanical strength for the extruded filament for maintaining the shape and supporting the next layers that are printed [5]. The improvement of the interfacial bonding strength between two printed layers may enhance the stackability of hydrogel as it prevents delamination within multilayer stacks [5,36].

Shear-thinning behavior can be characterized using rheology [121]. Shear rate sweeps determine the viscosities across a range of shear rates, i.e. the bioink's going through a nozzle can be mimicked by applying shear rates from low ($<10^{-3}s^{-1}$) to high ($>10^{2}s^{-1}$). For extrusion process, high viscosity at low shear rates and low viscosity at high shear rates is necessary. Materials with these characteristics are called shear-thinning. [19] Typical viscosity-shear rate graph is presented in Fig. 5 (a).

For comparison, the experimental rheological data should be fitted to pre-existing rheological models, such as Herschel-Bulkley (HB) model

$$\tau = \tau_0 + k\gamma^n, \tag{1}$$

where τ_0 is yield stress, τ is fluids shear stress, k is consistency index, γ is shear rate, and n is flow index, i.e. fluid has solid properties if $\tau < \tau_0$, whereas if $\tau > \tau_0$, it is shear thinning when $n < 1$ and shear thickening when $n > 1$ [119]. Another similar model is Power law model

$$\eta = K\gamma^{n-1}, \tag{2}$$

where η is viscosity, K is the flow consistency index, γ is shear rate and n is the shear-thinning index. It is used for materials with no observable low or high shear rate viscosity plateau. The degree of shear thinning can be described with n, i.e. when $n = 1$ it is Newtonian, $n < 1$ it is shear thinning, and $n > 1$ it is shear thickening. It has been shown that if $n =$ 0.3–0.4 the flow profile is appropriate for bioprinting. [19]

The difference between injectable and 3D-printable materials is that injectable materials only have to be shear-thinning, but bioinks for 3D-printing need to localize or stabilize at given point. When bioink has been extruded from the nozzle there are no or little shear forces exerted. It would be important to calculate the shear rates throughout the printing process and apply these shear rates in the rheological tests, as well as study the recovery of viscosity. [19] Shear rate is important to understand during the printing process, because hydrogel is extruded through a syringe to a narrow nozzle, which have different inner diameters. Based on fluid mechanics, non-Newtonian fluid's viscosity is a function of shear rate. If there is a constant volume flow rate, there is a change in the linear flow rate because the cross-sectional area of nozzle and syringe changes, leading to change in the shear rate. [5]

4.3. Shear-thickening and thixotropic properties, and Barus effect

Non-Newtonian fluids can also have thixotropic properties, which are quite similar to shear-thinning properties (viscosity-shear rate-plots look very similar), except that thixotropy is time-dependent unlike shear-thinning. This can be illustrated by plotting viscosity against time with constant shear rate (Peak hold test). Viscosity of thixotropic materials decreases with time, whereas viscosity of shear-thinning materials is constant. [19,31] For printing, this kind of behavior should be considered since it might lead to inhomogeneous dispensing and uneven distribution of cells or particles [31,32]. Therefore shear thinning materials are ideal because they are not time-dependent [32]. The previously mentioned peak hold test can simulate the printing conditions and help to assess printability. Fig. 5 (b) shows that, first the ink experiences a constant low shear rate (in the syringe), then endures a high shear rate (extrusion), and last relaxes back to a low shear rate (in air). Shear-thinning behavior enables the drop of viscosity during extrusion and bouncing back after removing shear stress. [122] Another test is a thixotropic loops test. After extrusion, the hydrogel's crosslinks broken by shear stress should self-recover, i.e. viscosity should quickly recover after shear rate is removed. [5] Rheological measurement where shear rate is first increased and then decreased in a set amount of time (thixotropic loops) can be used to show the rebuilding time of internal structure. If curves overlap, it indicates non-ideal bioink with minimal internal structure. If there is a difference in the loading and unloading curves, it indicates thixotropic behavior of a certain degree. However, the interpretation of this test is difficult and requires special "cup and cone" geometries. [19]

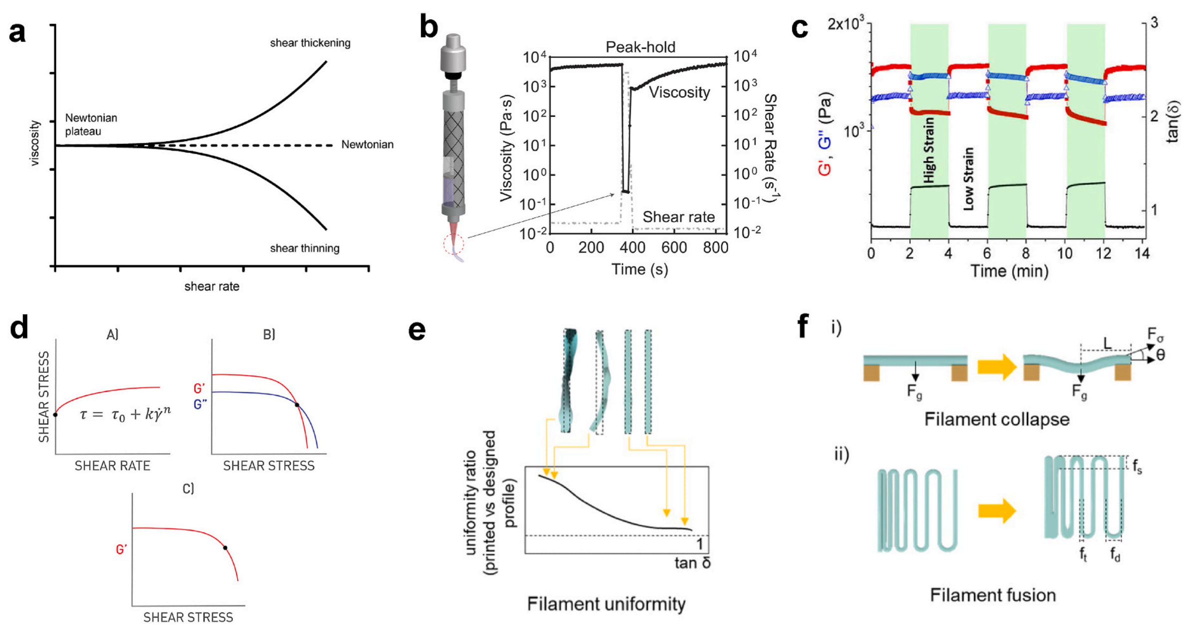

Fig. 5. Pre-printing characterization of bioink: (a) shear-thinning [31], (b) peak-hold test [122], (c) alternate step strain test [123], (d) yield stress (A) Herschel-Bulkley model, B) shear stress at the crossover point of G′ and G″, C) shear stress related to a pre-determined deviation of G′ from linearity (i.e. 85% deviation)) [119], (e) filament uniformity test [43], and (f) filament collapse (i) and fusion (ii) tests [43]. Reprinted with permission from Jungst et al. (2016) [31] Copyright © 2016 ACS Publications, Lee et al. (2022) [122] Copyright © 2022 Wiley Online Library, Ouyang et al. (2016) [123] Copyright © 2016 ACS Publications, Townsend et al. (2019) [119] Copyright © 2019 Elsevier, and Schwab et al. (2020) [43] Copyright © 2020 ACS Publications.

Another unfavorable property for 3D-printing is shear thickening, which is opposite of shear thinning, meaning that viscosity increases when shear rates increase. Like thixotropic is counterpart with shear thinning, shear thickening is counterpart with rheopectic which is opposite to thixotropic. [31] Shear thickening materials have higher viscosity under pressure so they clog the nozzle [32].

When designing the ideal bioink so called Barus effect should be considered. Barus effect, a phenomenon of extrudate swell, means that the jet diameter increases after material flows from the print head through the nozzle. This is true for elastic polymeric materials, i.e. polymer chains are stretched when material flows through the tube as it compresses by the given confinement. After ejection of material it expands because of the chain's elasticity and partial relaxation leading to increase of jet diameter. This phenomenon needs to be taken into account for high-resolution printing, i.e. optimizing process parameters (deposition speed) the compensation of the effect can be done to some extend. The Barus effect should be small or no effect at all for the preservation of resolution. [31]

4.4. Viscoelasticity and yield stress

Extrusion-based bioinks have both flow and shape retention properties. Viscoelasticity, meaning that material has both viscous (fluid flow) and elastic (elastic shape retention) characteristics when it undergoes deformation, can be used to describe this behavior. Two parameters i.e. storage modulus G' (shape retention) and loss modulus G" (viscous flow) can be measured for bioinks using oscillatory rheology. So called damping factor $\tan(\delta) = G''/G'$ can be used to identify a suitable balance between flow and shape retention. [43] Viscoelasticity protects cells from shear stress during the printing process [1]. Rheological properties, like inadequate G' of many soft hydrogels may also lead to the collapse of structure [25].

Shape retention can also be determined using yield stress. Yield stress (in fluid mechanics) is defined as the stress that is needed for fluid to begin to flow (i.e. stress that is needed for material to begin to deform under an applied shear stress). It quantifies the place where fluid is on the spectrum of paste to putty behavior. If yield stress is zero, it has traditional liquid behavior (flows upon exposure of stress), whereas increased yield stress gives paste or putty behavior, i.e. materials with lower yield stress easily flow for injection. Since the difference between paste and putty is not well defined, Townsend et al. have suggested 100–2000 Pa for paste and above 2000 Pa for putty materials. Precursor solutions with no or low yield stress can be used for injection through high gauge needles. [119] Yield stress should not be confused with apparent viscosity, meaning that apparent viscosity is related to the force needed to continue dispensing from the syringe after flow has begun. Yield stress, on the contrary, is contributing to material's injectability/syringeability (to generate flow initial force is required) and retention within the defect after placement (in the absence of applied force there is no movement). [119] In order to bioink to be printable, it must overcome a certain minimum amount of stress (yield stress) to be able to flow from barrel onto the printing bed. The weak network interactions of hydrogel precursors are interrupted when the applied stress is above yield stress. [19] Thus, yield stress gives basically the force that is needed for gel extrusion. It also gives indirect information about the gel strength since suitable yield stress enables the stacking of layers during 3D-printing, i.e. higher yield stress gels can support more stacked layers without printing defects compared with low yield stress gels. [124] For 3D-bioprinting applications, bioinks that exhibit a yield stress but have also shear-thinning behavior and fast recovery time, can resist deformation and maintain the printed structure. In order to get high shape fidelity, yield stress above 100 Pa is needed for proper layer stacking. [119]

Rheology can be used to study yield stress that tells about hydrogel precursor solution's retention at the defect site. Townsend et al. [119] have illustrated three ways to determine yield stress (Fig. 5 (d)), i.e. A) theoretical model fitting, e.g. Herschel-Bulkley model, B) shear stress at the crossover point of G' and G'', or C) shear stress related to a pre-determined deviation of G' from linearity (i.e. 85% deviation). [119]

4.5. Reversible interactions & recoverability

Shear-thinning and self-healing hydrogels suit for 3D-bioprinting due to liquid behavior during extrusion through nozzle and rapid solidification (structural recovery) after deposition [12,29]. Static hydrogels, on the other hand, cannot mimic the biological tissue's hierarchical complexity since the microenvironments are uniform and static. They also have limited structural complexity, large equilibrium volume swelling, and opaque and brittle nature. [29]

The dynamic inks can be divided into two category according to interaction type: via supramolecular interactions (e.g. hydrogen bonding, host-guest recognition, ionic interactions, hydrophobic interactions, $\pi - \pi$ interactions) or via covalent bonds (e.g. Diels-Alder reaction, thiol-ene chemistry, photoresponsive cycloadducts, imine, acylhydrazone). Depending on the interaction, the physical and mechanical properties as well as recovery time and recovery percentage will range. Currently, EBB, DBB and stereolitography have been used for the printing of dynamic inks. [29] EBB is the most commonly used for self-healing hydrogels. In EBB, printing the ink should be fluid like when going through the nozzle but should have enough structural integrity when it is deposited for the support of subsequent layers. Shear-thinning nature of these hydrogels enables this reversible action i.e. they can be printed after gelation and reform the 3D structure after to circumvent the limitations of gelation. [14] Reversible interactions of hydrogel can provide desirable mechanical properties (mechanical strength and elasticity) as well as enhance the shear-thinning which further improves the printability [18]. Shape fidelity can be improved by structure recovery after extrusion i.e. the sagging of the construct will be reduced and more room for post-crosslinking will be provided [25]. In order to achieve high resolution bioprinting, fast return to original properties is needed [119]. The recovery time and transition process is influenced by the interactions between the molecules. For printable systems the solidification conditions are more strict than for injectable materials due to shorter acceptable gelation time and smaller diameters of nozzle used for printing. [31] Recovery time can dictate how easily the cells can be incorporated, for example, too quickly recovered materials would result heterogeneous cell distribution since the mixing in cells is difficult. Also, too slow recovery time would result heterogeneous cell distribution, cell sedimentation and poor shape retention. Shape fidelity would be improved by using naturally quickly recovered materials. For bioprinting, relatively quick recovery time, i.e. 5-10 s (>85% of G') are recommended. It should be noted that after extrusion and recovery, the external forces like weight of stacking layers should be resisted by the bioink to prevent poor shape fidelity. [119]

Due to fabrication conditions of nozzle-based systems, shear thinning region and hydrogel recovery after printing should be known and therefore characterized [31]. Mechanical testing can be used to quantify self-recovery, i.e. cyclic loading/unloading in tension, compression or shear can be used. In strain-relaxation experiments (i.e. alternate step strain measurements, Fig. 5 (c)) the hydrogel is exposed to a constant deformation (strain) in a stepwise manner over a period of time. Thus, the viscoelastic response of material to damage (decrease of G') and internal crosslinks' reversibility (recovery of G' and G"; percentage of recovery) are revealed, as well as the lifetime of the reversible interactions (recovery time). There has also been a similar tests tracking the viscosity with changes in shear rate. [14] In addition to this, in case of dynamic inks, a full characterization of self-healing would be recommended as Karvinen et al. [121] suggest.

4.6. Filament formation and shape fidelity

Shape fidelity refers to printing quality which tells how well the bioprinted structure matches the original model [119]. High shape fidelity and large vertical height are desired characteristics in 3D-bioprinted construct. Shape fidelity is needed for the maintaining of extruded filaments' shape and supporting the printed structure (pores and channels). [5] High fidelity of cell-laden printed construct should also be ensured by the bioink after and during the bioprinting so that resolution, size, structure and shape stability are maintained for a desired time (e.g. over a period of cell culture) [1,11]. High shape fidelity can be achieved by balancing material's shear-thinning, recoverability and yield stress properties. Bioink's swelling behavior, determined by the charge densities and extend of crosslinking, is also affecting to shape fidelity, i.e. lower swelling ratio with high crosslinking density provides high shape fidelity, although reduces diffusion of nutrients and oxygen. [19,26] Good shape fidelity can also be achieved by combining two hydrogel materials, first one providing enhanced cell activity and other mechanical stability [19]. Structure recovery after extrusion can also improve shape fidelity i.e. the sagging of the construct will be reduced and more room for post-crosslinking will be provided [25]. Supporting bath system in bioprinting has also been found to improve shape fidelity [5]. Further, it has been found that as size of the construct reduces, the accuracy decreases. In order to improve print resolution and shape fidelity, print paths (height and/or width) should be manipulated and controlled. Optimization of the printing process can be done by improving the print resolution by using smaller nozzle diameters, and using lower extrusion rate. [11]

In addition to previous pre-printing rheological characterization (yield stress, shear-thinning, shear recovery) of bioink to assess their flow initiation and extrudability i.e. continuous linear filament formation in air, fiber formation and stacking ability can be used to assess the shape fidelity and uniformity of single lines. Uniformity of filament can be assessed via image analysis (e.g. light microscopy or micro-computed tomography (micro-CT)) and quantified by the loss tangent (tan δ), i.e. higher value correlates with better filament uniformity (Fig. 5 (e)). Since the printed filaments can also deform under different forces, like gravity and surface tension, their ability to counter gravity can be tested by printing a filament over a pillar array (increasing distances) and estimate it by measuring so called deflection angle θ, or analyze filament fusion (due to surface tension) by printing parallel structures/filaments with narrowing filament spacing (Fig. 5(f)). [43]

There are also quantitative tests to study the bioink's shape fidelity during and post-printing. Like Fig. 6 (a) shows, the homogeneity of single filaments can be assessed based on the fiber diameter (homogeneous filament if $d_1 = d_2 = d_3$) [43]. So called expansion ratio (i.e. spreading ratio)

$$\alpha = d/D, \tag{3}$$

where d is printed filament diameter and D is nozzle diameter, that indicates the material's flowability on the base it is deposited once printed, and uniformity factor

$$U = \frac{\text{length of the printed structure}}{\text{length of the theoretical design}}, \tag{4}$$

can also be determined [125]. For example, Maiz-Fernandez et al. [125] showed that the expansion ratio increases when printing speed decreases and extrusion pressure increases. Further, the uniformity factor decreases when printing speed increases, whereas at lower speeds the factor is close to 1 giving best precision. [125]

With planar structures (Fig. 6 (b)), filament diameter and merging (intersection/overlay of two filaments) can be evaluated, as well as transversal pore geometry. [43] In the last case, ideal filament stacking with optimal rectangular pore shape and interconnected channels can be obtained with printability index Pr = 1 [11,43]. This is a semi-quantitative evaluation based on the shape fidelity of the pore and circularity of printed filaments [43]. Pr can be evaluated by calculating

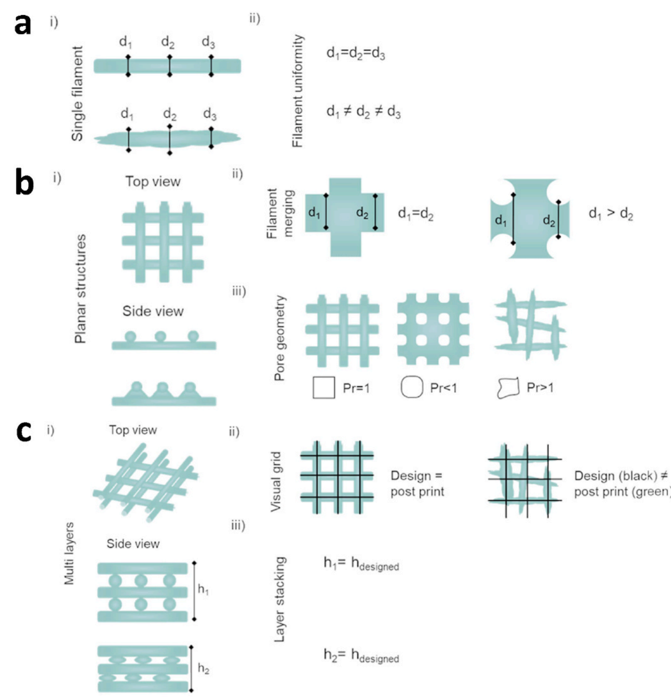

Fig. 6. During and post-printing characterization of bioink: (a) homogeneity of single filaments, (b) top and side views, filament diameter and merging, and pore geometry (ideal filament stacking with Pr = 1) of planar structures, and (c) top and side views, visual grid (indicating matching of printed structure with computer designed shape), and layer stacking (indicating shape retention of circular filaments) of multilayered structures. Reprinted with permission from Schwab et al. (2020) [43] Copyright © 2020 ACS Publications.

$$Pr = \frac{\pi}{4}\frac{1}{C} = \frac{L^2}{16A}, \tag{5}$$

where C is the circularity of the print, L is the length, and A is the area. Pr<1 means poor fidelity, large and spreading curved corners and under gelation. Pr ~1 means print that matches the model design exactly, has exact material deposition with smooth prints and precise angles and has proper gelation, whereas Pr >1 means bioink has over gelation and has become rough or jammed, and print is poorly constructed with cracks and ridges. [11,19,126]

Multilayered constructs' (Fig. 6 (c)) shape fidelity can be analyzed post-printing by adding a visual grid that shows how well the printed structure (green) matches with the computer designed shape (black). Also, layer stacking (shape retention of circular filaments) can be evaluated with integrity index, i.e. by comparing the maximal height (h_1 and h_2) reached with the computer designed sample's height. Integrity index = 1 indicates high shape fidelity with optimal layer stacking, whereas if integrity index <1 filaments are merging and/or collapsing. [43] In addition to these, however, there would be a need to develop an approach to study 3D printability [19].

4.6.1. *Computer simulation and modeling of printability*

As previously stated, printability could also be semi-quantified using mathematical models or quantified using computational analysis [11]. Some examples are finite element analysis (models to simulate the mechanical behavior of the printed structures under different loading conditions, can predict potential failure modes [127]), computational fluid dynamics (simulates the flow of bioinks through the nozzle to optimize printing parameters, such as flow rate, pressure, and nozzle diameter [128]), or agent-based modeling (models the behavior of individual cells within the printed tissue to optimize the design of the printed structures and predicts their behavior *in vivo* [129]). In addition, sensory-based real-time monitoring systems and closed-loop feedback control algorithms are useable tools. For example, Yang et al. [130] quantitatively evaluated and monitored real-time the bioprinting process using high-speed, wide-field and full-depth imaging technique (optical coherence tomography) in association with the extrusion-based bioprinter (3D P-OCT). This method provided *in situ* multi-parameter (e.g. layer-to-layer thickness (LT), filament size (FS), and pore size (PS)) monitoring, as well as further quality evaluation with multiple volumetric parameters (e.g. material volume (MV), volume porosity (VP), and pore connectivity (PC)). Since this method provides real-time monitoring of the printing process and feedback in a timely manner, printed constructs with better structural fidelity, functionality, higher spatial resolution and design complexity could be achieved. [130] An example of the latter, Li et al. [131] proposed a novel closed loop feedback control algorithm, by using digital holographic microscopy (DHM)-based stiffness imaging feedback, to control the photopolymerization of hydrogel bioink and hence the mechanical stiffness and print fidelity. The adjustment of the photocuring degree and further the crosslinking density was allowed by the DHM-based stiffness imaging feedback in every grid area, leading to large-span and high-resolution modulation of mechanical properties. Thus, complex biomimetic structures with modulus gradient can be achieved. [131] In conclusion, computational modeling in conjunction with sensory-based real-time monitoring systems and closed-loop feedback control algorithms can be used to optimize printing conditions and to improve the quality of bioprinted constructs.

4.7. Surface tension

Bioink's surface tension influences to resolution, printing quality and printed line width. For example, surface tension can affect to printability, as it can cause the collapsing of the printed structure. It can also lead to nozzle clogging as it can cause the bioink to adhere to inside the nozzle. It has been found that printed constructs expand outwards not inwards maybe due to preventing action of surface tension on the inner walls. It has been actually proposed that constructs should be printed thinner compared with target size, so that the size of the final expanded construct matches with native model. [11,132] Surface tension can also affect to printed cells' viability as it can cause mechanical stress during printing. The surface tension is inversely proportional to the bioink's cell concentration as more cells can be absorbed to the liquid-gas interface [3]. Many times, the effect of surface tension of printability has been neglected in literature. It is not only important for DBB, but also for EBB. [132]

4.8. Crosslinking properties

The formation of stable construct structure is determined by the crosslinking chemistry (usually secondary crosslinking for stabilization) [10,19]. The as-printed filament's consistency and viscosity should allow the quick gelation or restoration once printed in order to keep the filament's outline as a circle (cross-section) [36]. The fixation i.e. gelation of hydrogel minimizes the structure collapse by preserving the shape for the construct [26]. The rate of gelation, on the other hand, is determining the printing speed. However, the gelation kinetics and its direct relation to printability and printing speed need more studies. [25] Hydrogels can be fabricated through physical and chemical crosslinking. Physically crosslinked hydrogels lack good mechanical properties that can cause stability issues and difficulties in handling of the construct. Therefore chemical crosslinking can be used to stabilize the construct after printing. For example, a hydrogel with dynamic supramolecular bonding (self-healing), having shear-thinning and supporting properties can be stabilized with covalent crosslinking (UV induced), enabling direct printing on the ink into self-healable structures (multimaterial complex construct). [1] Since physically crosslinked hydrogels are often unstable they are more suited to function as fugitive sacrificial templates with temporal stability, whereas chemically crosslinked hydrogels with longterm stability are suitable for constructive bioprinting [10]. It should also be noted that different fabrication strategies are needed for different bioink materials due to their different crosslinking mechanisms and rheological properties [41]. Additionally, it is also important to determine the crosslinking mechanism's cytocompatibility as cells are encapsulated during the process [1].

4.9. Interconnected pore structure

Construct with interconnected pore structure is desired. Structure parameters, such as mesh size, crosslinking density, pore size and distribution, pore shape and orientation, specific surface area, pore interconnectivity, etc, should be optimized for cells, transfer of oxygen, waste etc., and tissue integration [1,133].

4.10. Mechanical properties

Mechanical integrity and elastic moduli are biomechanical attributes of printed construct [19]. For example, suitable stiffness makes sure that the construct can self-support, as well as directs and controls the cell behavior [2,36]. Reinforcement of hydrogels can be made by adding a dissipation mechanism (e.g. reversible crosslinks) into the networks as well as with maintenance of high elasticity (e.g. interpenetrating long chain networks, crosslinkers with high/hybrid functionality, macro/-meso composites) during deformation. In addition to bioink's mechanical properties the mechanism of reinforcement affects to its strength, recovery behavior and flow, and further to printing resolution and structural integrity. [25]

Characterization of mechanical properties using compression or tensile test tells whether bioink has a ability to withstand deformation. As a note, traditionally, compressive modulus has been determined from the slope of the stress-strain curve, which does not account the fact that with hydrogels the stress-strain proportionality is not linear and cannot be determined this way. One possibility would be to use an alternative polynomial-based approach proposed by Karvinen et al. [134]. The mechanical properties of printed structures can be compared with bulk properties. As expected they are different due to low polymer alignment of cast hydrogels compared with layer-by-layer printed hydrogels that may have void spaces or aligned polymers. In ideal case, there is a 100% layer adhesion and contact with printed sample. It should be noted that if circular gauged nozzle is used, geometric mismatch may lead to some space where cracks may propagate and thus lead to decreased compressive modulus. [19] Like said, interfacial defects in layer-by-layer printing can lead to poor stackability and constructs that are mechanically weak [5]. The deposited bioink layers should adhere to each other in order to form structure that is mechanically rigid. Delamination of layers (due to low adhesion) may result a defect leading to possible crack propagation and stress concentrators. [19] To characterize this, a lap-shear test has been used to study multilayered hydrogel structures' interfacial bonding. Shortly, fractured surfaces are created by pulling the samples apart across their surfaces until failure are observed. The interfacial failure indicates the interfacial adhesion between the two layers in a layered construct. Ultimate shear stress (USS), obtained from the lap-shear measurement, can also be used to indicate adhesion properties, i.e. how the sample can resist failure in shear [5]. To study the multilayered hydrogels after printing, Fuentes-Caparrós et al. [135] have introduced a rheological protocol (using vane and parallel plate geometries), which allows to measure the properties at different depths (each layers), but also determine what is the contribution of the neighboring layers, and whether they affect to bulk properties of the construct. Fuentes-Caparrós et al. showed that in their example case printing process heavily influenced to the hydrogel properties. [135] Previously, for example, Nie et al. [136] and Nguyen et al. [137] have also studied mechanical properties of multilayered hydrogel constructs, but only focused on individual layers.

4.11. Swelling

Swelling happens after bioink crosslinking and placing into cell culture media or implanted site. Swelling, as amount of fluid increases, can increase the distance between the net points or crosslinks and decrease the crosslinking density, and thus also affect to mechanical properties of the printed structure. [19] Absorption of fluids and contraction can lead to closing of vessels or pores. If multiple materials are used with different swelling/contractile behavior, it may lead to layer integrity loss or final construct's deformation. [6] The positive thing with swelling is the allowing of therapeutics or waste products diffusion [19].

4.12. Degradation

The printed (cell-laden) constructs should be stable under the *in vitro* or *in vivo* conditions up to a desired time scale in order to give support for the cells until they produce their own ECM proteins [2,5]. However, it should be noted that at the same time cells' physiological environment changes as the mechanical strength reduces [25]. Bioink's composition and concentration, temperature and cell culture media determine the printed constructs degradation rate [2,5]. The degradation rate could be modified, for example, by combining hydrophilic and hydrophobic polymers [25]. The chose of hydrogel with suitable degradation rate should be done based on the intended tissue types [2,5]. Non-toxicity (with no inflammatory response) of the degradation products (and bioink) is also necessary since it defines the biocompatibility of the construct. Toxic byproducts can be either small molecules or proteins, but also temperature or non-physiological pH. [2,5,6] Changing temperature conditions may influence to printed construct if thermosensitive hydrogels are used [5].

4.13. Polymer origin

Hydrogel materials used for 3D-(bio)printing inks are natural and/or synthetic based. Natural polymer based (e.g. collagen, alginate, fibrinogen, hyaluronic acid etc.) have similarity to human ECM, self-assembling ability, and are inherently bioactive and biodegradable. Synthetic polymer based (e.g. polyethylene glycol (PEG), polyacrylamide etc.), on the other hand, are tailorable by their physical properties for the application, and stimuli responsive (pH, temperature), have robust mechanical properties, photo crosslinking ability, and controllable degradation time, however they have poor biocompatibility and non-natural/toxic degradation products. [6,22,42,138] In order to meet the requirements of ideal ink, modified natural polymers are often mixed/modified with synthetic polymers for appropriate shear-thinning and viscosity [36]. Further, the materials used for hard and soft tissue differ from each other, for example, bone might need additive bioactive ceramics (hydroxiapatite etc.), whereas skin would need hydrogel materials, such as hyaluronic acid or collagen [41]. Regardless what polymer is used, crosslinking density and molecular weight are the most critical characteristics influencing cell behavior. For example, cell proliferation, migration and formation of tissue are aided by lower crosslinking density as nutrient diffusion and removal of wastes are facilitated. Natural based polymers have high molecular weights whereas the molecular weights of synthetic polymers can be customized. Stiffer gels can be achieved with higher bloom strength. Molecular weight affects how much gel can undergo swelling which affects to supplementation of nutrients etc. It also controls flow characteristics of bioink as well as the biocompatibility and mechanical properties. Printability can be improved by increasing crosslinking density, molecular weight or concentration, although it limits the cell migration and reduces nutrient diffusion. Further, if polymer dispersity index (PDI = molecular weight distribution) is low similar length polymer results in consistent mechanical properties. Synthetic polymers are usually less polydisperse than natural polymers. Degradation also affects to polymer selection. [19]

4.14. Cellular biocompatibility

Pre- and post-printing high cell viability together with cytocompatibility and biocompatibility are important for ink formulation. Bioactivity can be added through functionalization with bioactive molecules, although this may change the shear-thinning behavior and mechanical properties and need optimization before printing. [2,18] Cellular biocompatibility should be estimated in order to understand cell-bioink interactions and how bioink can stimulate cells [19]. Also, shear force and degradation byproduct effects on the bioprinted system, as well as concentration-dependent effects of nanoparticles on cells, and effect of printing pressure and polymer crosslinking agents on cell viability should be estimated [19,139,140]. Different cytotoxicity and viability assays can be used. Drawback of the methods is that they concentrate only on cell viability and not for example on differentiation of cells or protein secretion. RNA-sequencing could be used although it is time-consuming and expensive. [19] Together with viability, also cell proliferation, differentiation and adhesion should be studied. The measurement of cell-material interactions is usually done by 2D seeding cells on the surface of bioink, but 3D cell encapsulation measurements, although being more complex, would provide better knowledge since they mimic the *in vivo* microenvironment. Initial cell screenings should be done when designing new bioprinting bionks. [19,141] The traction force between materials and cells can be studied using traction force microscopy (TFM) if bioink is transparent and has flat surface [19,142]. Alternatively, vinculing staining can be used to elucidate cell binding and see focal adhesion points [19,143]. In 3D TFM, cells do not have to be on the exterior of the sample for analysis. It provides information about behavior of cells in 3D cultures. However, rheological properties of bioink may be altered due to incorporation of fluorescent beads. [19,144] Atomic force microscopy (AFM) can be used to quantify how strongly cells can adhere to the bioink surface and both cell-matrix and cell-cell adhesion forces can be measured [19,145]. However, this technique cannot sense fully encapsulated cells unless the printed construct is destroyed [19,146]. Cell-matrix interaction can also be studied using multiple particle tracking microrheology (MPT) [19,147]. The cell behavior can be understood better by quantifying the deposited matrix and proteins. This is important in bioprinted constructs since they could mimic the native tissues' 3D architecture. There are different methods to quantify different components, for example, collagen can be quantified by quantifying sample's hydroxyproline or using dyes such as Sirius Red F3BA. [19] GAGs (hyaluronan, heparan sulfate, chondroitin sulfate, dermatan sufate, keratan sulfate) can be quantified by using Alcian Blue and Dimethylmethylene Blue (DMMB) assays [19,148].

Post-printing incubation of printed cell-laden constructs can be done either statically in cell culture, or dynamically in bioreactors which provide continuous infiltrating medium flow, and for example compressive/tensile load [23]. In later case, rapid post-printing maturation is allowed by using new bioreactor techniques that would provide mechanical and chemical stimulation that assist tissue remodeling and growth [3]. In fact, bioreactors can be used for the maintaining of tissue construct's viability and post-processing functions, and can be combined with innervation and angiogenesis promoting factors and with cell viability maintaining and preserving factors. In addition, microenvironmental parameters such as pH, temperature and gas and nutrient concentrations, but also mechanical stimulation regulation can be maintained. [6]

5. Challenges and future prospects of 3D-bioprinting

Despite the great advances in 3D-bioprinting already, there still remains some challenges to overcome. The selection of scaffold material, formation of printed constructs, biomechanical control, assurance of aseptic environments, nutrient transport, blood supply, and long-term survival of construct can be considered as general challenges of 3D-bioprinting (and ink materials). [8] In terms of inks, weak interlayer adhesion of the printed polymers, increased processing speed triggering polymer's rheological phenomena or using static inks are challenges that influence to mechanical properties, printability and shape fidelity [29]. Currently, there is still a lack of diversity in biomaterial inks. The properties of many printable material are suitable for external applications, but in the case of implantable biomaterials, physiological conditions and body interactions make their design more difficult. It has been already stated that hydrogels intended for 3D-bioprinting should be printable, biocompatible, have suitable mechanical properties and degradation kinetics, form safe degradation byproducts, as well as biomimic tissue. However, it is known that many of previous characteristics are opposing. [138] For example, in case of high-strength hydrogel inks the challenges are how to make biocompatible inks with proper degradability, ability to integrate with tissues and cell affinity, as well as multi-level gradient structures having continuous anisotropy. Further, developing of new printing strategies, like combining different printers/methods to print high-strength scaffolds with micro/nano-multi-scale structures would be needed for more complex tissues/organs. [36]

3D-bioprinted construct for soft tissue regeneration should be biomimicking, i.e. not only possess complex structure of human organ, but also have suitable mechanical properties, porosity, pore distribution and interconnectivity, flexibility as well as recovery rate. To meet these needs, multilayered structures should be designed and fabricated. [4] When designing scaffolds and tissue constructs, it should be noted that different cell types behave differently depending on the architecture, for example, high porosity is needed for effective media transport in case of metabolically active cells like cardiac cells, whereas for cell types with hypoxic environment, like chondrocytes, less porous architecture is better [41]. There will also be a need for larger tissues and organs. When the size of the printed tissue/organ increases, the transportation of nutrition and oxygen becomes more important for maintaining cell viability and tissue maturation leading to need of successful vascularization [28]. Innervation, on the other hand, is needed for proper function and integration of implanted constructs with the host tissue, and is intricately linked to vascularization [107]. However, still many 3D-bioprinting studies focus either on neuronal generation or vascularization, but a combination of these features should be considered and studied more [149]. One limiting factor has been how to supply an universal medium to both vascular cells and neurons (as well as corresponding support cells) that can sustain both phenotype development and maturation [150]. The challenge of current 3D-bioprinted constructs is the lack of controllable micro-environment, i.e. only submicron level resolution is possible. Therefore, more heterogeneity with hierarchical or functionally-graded properties is needed. Also, using soft materials like hydrogels (and cells) as a bioink, the retaining of shape after printing may be difficult due to, for example dehydration, swelling or contraction. [41] In case of stem cells, the challenge in bioprinting of them is slow fabrication rate, for example currently full human liver would take 3 days print, which would reduce viability of stem cells. Other challenge is the delivery of cell concentration that matches physiological packing of tissues, for example currently only up to 10^7 cells/mL can be printed, while 5 to 10×10^8 cells/mL density would be considered suitable for sufficient for tissue and organ function. [20] Moreover, the progress towards clinical translation is currently hindered by the lack of comparability of bioprinting studies, i.e. there exist differences in cell culture protocols as well as cell line sources used between studies. For example, standardized protocols for biocompatibility quantification of cell seeding density or additives influencing on rheological property are not well known. If you think about the end application, biocompatibility and cytocompatibility are as important as printability. [151] One challenge is also how to ensure that the printed tissue has consistent composition, structure and function. Thus, the printing process should be optimized, and the printing parameters should be controllable, which further ensures required reproducibility. [152] The high cost of the printing process and time needed, for example, for model creating processes is still also a challenge [152]. Regulatory approval should also be considered. It is needed before EBB can be used in clinical applications. Currently, there is a lack of laws and regulations for bioprinting (e.g. bioprinted tissues and organs), although, recently US FDA has released a guidance on the regulation of 3D-printed medical devices [153], which in future may act as a regulation framework for bioprinted tissues and organs. It should also be noted that majority of clinical trials have been made on animals, which will raise ethical concerns as we move to transplantation of tissues to humans [154]. Currently, there are no ongoing clinical trials, for example, for bioprinted cell-laden cartilage, bone, cardiac, central/peripheral nervous systems, skeletal muscle, or kidney tissue/organ constructs (ClinicalTrials.gov). However, for example in case of skin grafts, there are already some companies (e.g. Poietis, Cellink/BICO, ROKIT Healthcare) working on commercializing 3D-bioprinted functional skin. Anyway, EBB has a great clinical potential since it can be used to create customized tissues and organs for specific needs of patients. EBB can print different kinds of cells and materials, which could be tailored so that specific biomimicking complexity as well as chemical, mechanical and biological properties are achieved, which further would ensure proper integration with the host tissue. All in all, the translation of EBB into clinical practice is still in a beginning due to those challenges mentioned above that need to be overcome. Once these challenges are overcome, EBB will have great potential in regenerative medicine. For transplantation, patient-specific tissues and organs can be created to reduce the need for donor organs or the risk of rejection. At that point, the bioink design is no longer about its feasibility for bioprinting or to ensure cells' activity, but about how to promote cells' functionality so that the clinical use of printed tissues and organs is possible and tissue damage can be repaired [154].

In terms of characterization, for example, even if standardization of bioink printability (effect of rheological parameters on final resolution) is already in progress currently there are no standardized method to define resolution [151]. There are different parameters used to describe it, but for the future standardization would be needed in order to compare the printing methods better [19,26]. Computational modeling in conjunction with sensory-based real-time monitoring systems and closed-loop feedback control algorithms, on the other hand, could improve the 3D-bioprinted construct design and quality as they allow optimization of the printing conditions, as previously shown in Chapter 4.6.1. For example, by using closed-loop controlled path planning for 3D-(bio)printing, the requirement of an initial description of part geometry could be avoided as it enables real-time sensing and control of nozzle-surface offset [155]. In order to get better simulation results, the synergistic response between the materials and cells should also be characterized [9,156]. Simulation of product performance can also give ideal time point when printed construct should be implanted [9,157].

Technological challenges of 3D-printing, like increased compatibility with biologically relevant materials, and increased speed and resolution, should be overcome by designing new more suitable 3D-bioprinters. Thus, the extension of range of compatible materials as well as methods how to deposit the cells and materials more precisely and specifically would be possible. Fabrication speed must be increased in order to fabricate clinically relevant sized constructs. One possibility is using miniature functional blocks that can be joined to fabricate macro-scaffolds. [6] Also, microvascular multinozzle printing has been proposed as a fabrication methods for large-scale constructs with multiple components or hollow structures to minimize the fabrication time [24]. There are also printing technique specific challenges. For example, in case of EBB, additional compensation in the z-axis is needed since many hydrogels contract in z-axis during bioprinting. Also, the distance between the printing plane and nozzle tip may increase over time leading to imperfections/failures, which could be overcome by using automatic adjustment of the distance during printing. To overcome the challenges of using soft hydrogel bioinks can be done by using bioprinting of hydrogel into a hydrogel bath described earlier. [41] In case of DBB, the challenge is how to control number of cells encapsulated in a droplet, and the droplet volume and their placement, in order to print high resolution tissues with even amount of cells. Bioink rheological properties should be tuned so that they can protect cells from shearing forces, but also nozzle geometry should be altered in order to print sub-micron to micrometer resolution with higher viscosity inks as it restricts viscosity of bioink and droplet size. Overall, print-heads and nozzles should be tuned to overcome their current restrictions. [22] For future applications, inkjet printing needs to be combined with other printing techniques due to its limitations related to viscosity or vertical printing [23]. The challenge with LAB is the positioning of bioink only onto a prefabricated scaffold, but it is also expensive method. On the other hand, EBB has fast fabrication time for larger structures, but the cell survivability is poor. Thus, combining these methods together could give better constructs with physiologically relevant proportions and support of cell viability. [23] In general, printing modalities should be more accessible. Also, the cost of bioprinters should be lower so that they would be more available for broader users in science. In future also development of hybrid bioprinting systems that could dispense multiple materials, cell populations and biochemical cues (drugs, growth factors and nutrients) are anticipated. [19]

Thus, the future of 3D-bioprinting is going towards fabrication of patient-specific, and larger multifunctional tissue/organ grafts (complex heterocellular tissues including also multi-scale vascularization and innervation) and drug delivery systems [1,3]. Combination of multiple printing techniques together would permit reduction of production period and addition of complexity to architecture and function. Of course, the development of new printing techniques and instruments will advance 3D-bioprinting, for example, if external magnetic, acoustic or electric field would be applied during the printing, functional nanoparticles within the 3D-bioprinted construct could be assembled, distributed, aligned and oriented. Multimaterial 3D-bioprinting, on the other hand, could lead to creation of functional constructs with gradient, anisotropy, heterogeneity and complicacy. [1] The challenge of 3D-bioprinting considering only the initial state of the printed structure and assuming it as static and unchangeable, ie. assuming that printed cells form rapidly, assemble tissues and start synthesizing ECMs and thus provide/maintain shape and mechanical properties, could be overcome by adding time as fourth dimension aka using 4D-bioprinting [158]. Time means that the construct could adapt and transform to the new micro-environment and a range of physico-chemical cues over time after printing [11,158]. The structure can change when exposed to external (e.g. heat, light, moisture, magnetic field etc.) or intrinsic (e.g. cell forces) stimulus [1,19]. 4D-bioprinting would improve print resolution and modify the construct at molecular scale [11]. Basically, by using 3D-bioprinting one might mimic native tissue's complex architecture and microenvironment, but using 4D-bioprinting also the dynamic characteristic of complex organs could be achieved [25]. There are, however, challenges in 4D-bioprinting, for example responsiveness of stimuli-responsive materials can be affected by the cells, or material dynamics may reduce cell viability. Also, current stimuli-responsive materials response to only one stimulus, but in the body cellular activities are complicated and multiple stimuli control them. Therefore, designing 4D-bioprinted constructs able to respond to multiple physiological cues should be done. [7] With this in mind, supramolecular hydrogels with reversible crosslinks and stimuli responsive nature are one of the most potential candidates to be used as a bioink for 4D-printing [2,31,42]. Taylor et al. [14] have actually collected a table of possibly 4D-printable self-healing hydrogels based on their formation method (crosslinking type and gelation time), injectability, self-healing ability and suitability for reactive printing [14].

Further, in addition to 3D cell culture and *in vitro* disease models (tissue or organ models, vascularized models) studied already in the field of tissue engineering, some microphysiological platforms i.e. biomimetic microfluidic devices (tissue-on-a-chip and organ-on-a-chip) composed of *in vitro* 3D cell culture models in controlled perfusable microphysiological systems mimicking functions and biological features of native human tissues, organs and circulation have also been introduced [1]. 3D-bioprinting combined with those microfluidic systems would provide even more versatile and diverse designs of tissue/organ-on-a-chip systems (3D *in vitro* disease model), since the cells, ECM, biomaterials and growth factors can be spatiotemporaly placed within the engineered scaffold in order to mimic the native tissue or organ better [1]. Such systems can monitor cell activity as a function of time for 3D-bioprinted construct. The cell growth and function monitoring would give better understanding of the intra- and intercellular phenomenon and how efficiently bioinks can support such interactions. Thus, the development of functional tissues and organs for implantation would also go further. [38] Drug discovery and testing have also a shortage of tissue models [2]. The aforementioned systems would also work for the high-throughput drug trial and screening, and would replace the current animal and 2D cell culture models (*in vitro* drug testing) [1,22].

6. Conclusions

3D-bioprinting has become a valid technique to regenerate tissues and organs, because the printing of living cells is allowed while the hydrogel-based ink material provides mechanical and structural support to them. Among hydrogel-based inks, self-healing shear thinning hydrogels are most promising ink materials for EBB, because the ink can be extruded due to the decrease in viscosity under shear, and self-healed after removing the shear, which guarantees safe printing of cells and shape fidelity after printing. To achieve the best final bioprinting result, some printing technique, ink material and biological aspects of bioprinting need to be considered. In addition, the versatile characterization of pre- and post-printing properties of inks helps to improve the final bioprinted constructs. Despite the great advances in EBB and 3D-bioprinting in general, ink related challenges such as opposing characteristics, and lack of controllable micro-environment, or technological challenges such as need to increase printing speed and print resolution need to be resolved. In terms of characterization, more standardization is also needed. Additional computational modeling would also help to enhance the construct performance. Thus, the future of 3D-bioprinting is going towards patient-specific and larger multifunctional tissue/organ grafts with multi-scale vascularization and innervation. Probably multiple printing techniques need to be combined, but also new types of techniques are needed, for example applying of magnetic field during printing. Multimaterial bioprinting, on the other hand, would enable gradients and heterogeneity to the bioprinted structure. By using 4D-bioprinting, the dynamic nature of complex organs could also be added to the construct. Further, 3D-bioprinting, combined with microphysiological platforms, i.e. tissue- or organ-on-a-chip systems, would provide more versatile and diverse designs for them, but would also bring the development of functional tissues and organs for implantation forward. The translation of EBB into clinical practice is still in the early stages, but EBB has a great potential in regenerative medicine after the challenges, such as biomimicry, reproducibility or up-scaling related issues have been overcome.

Declaration of competing interest

The authors declare that they have no known competing financial interests or personal relationships that could have appeared to influence the work reported in this paper.

Data availability

No data was used for the research described in the article.

Acknowledgements

This work is supported by Academy of Finland (Center of Excellence in Body-on-Chip Research, CoEBoC decision number: 336663 (1.5.2020–31.12.2022)).

References

[1] J. Li, C. Wu, P.K. Chu, M. Gelinsky, 3D printing of hydrogels: rational design strategies and emerging biomedical applications, Mater. Sci. Eng. R Rep. 140 (2020), 100543.
[2] S. Ji, M. Guvendiren, Recent advances in bioink design for 3D bioprinting of tissues and organs, Front. Bioeng. Biotechnol. 5 (2017) 23.
[3] A.N. Leberfinger, S. Dinda, Y. Wu, S.V. Koduru, V. Ozbolat, D.J. Ravnic, I. T. Ozbolat, Bioprinting functional tissues, Acta Biomater. 95 (2019) 32–49.
[4] J.E. Kim, S.H. Kim, Y. Jung, Current status of three-dimensional printing inks for soft tissue regeneration, Tissue Eng. Regen. Med. 13 (6) (2016) 636–646.
[5] H. Li, C. Tan, L. Li, Review of 3D printable hydrogels and constructs, Mater. Des. 159 (2018) 20–38.
[6] S.V. Murphy, A. Atala, 3D bioprinting of tissues and organs, Nat. Biotechnol. 32 (8) (2014) 773–785.
[7] J.M. Unagolla, A.C. Jayasuriya, Hydrogel-based 3D bioprinting: a comprehensive review on cell-laden hydrogels, bioink formulations, and future perspectives, Appl. Mater. Today 18 (2020), 100479.
[8] S. Zhang, H. Wang, Current progress in 3D bioprinting of tissue analogs, SLAS Technol.: Transl. Life Sci. Innov. 24 (1) (2019) 70–78.
[9] J.M. Lee, W.Y. Yeong, Design and printing strategies in 3D bioprinting of cell-hydrogels: a review, Adv. Healthc. Mater. 5 (22) (2016) 2856–2865.
[10] Y.S. Zhang, K. Yue, J. Aleman, K. Mollazadeh-Moghaddam, S.M. Bakht, J. Yang, W. Jia, V. Dell'Erba, P. Assawes, S.R. Shin, et al., 3D bioprinting for tissue and organ fabrication, Ann. Biomed. Eng. 45 (1) (2017) 148–163.
[11] S. Kyle, Z.M. Jessop, A. Al-Sabah, I.S. Whitaker, 'printability'of candidate biomaterials for extrusion based 3D printing: state-of-the-art, Adv. Healthc. Mater. 6 (16) (2017), 1700264.
[12] L. Shi, P. Ding, Y. Wang, Y. Zhang, D. Ossipov, J. Hilborn, Self-healing polymeric hydrogel formed by metal–ligand coordination assembly: design, fabrication, and biomedical applications, Macromol. Rapid Commun. 40 (7) (2019), 1800837.
[13] Y. Tu, N. Chen, C. Li, H. Liu, R. Zhu, S. Chen, Q. Xiao, J. Liu, S. Ramakrishna, L. He, Advances in injectable self-healing biomedical hydrogels, Acta Biomater. 90 (2019) 1–20.
[14] D.L. Taylor, M. in het Panhuis, Self-healing hydrogels, Adv. Mater. 28 (41) (2016) 9060–9093.
[15] M.H. Chen, L.L. Wang, J.J. Chung, Y.-H. Kim, P. Atluri, J.A. Burdick, Methods to assess shear-thinning hydrogels for application as injectable biomaterials, ACS Biomater. Sci. Eng. 3 (12) (2017) 3146–3160.
[16] M. Guvendiren, H.D. Lu, J.A. Burdick, Shear-thinning hydrogels for biomedical applications, Soft Matter 8 (2) (2012) 260–272.
[17] A. Pal, B.L. Vernon, M. Nikkhah, Therapeutic neovascularization promoted by injectable hydrogels, Bioact. Mater. 3 (4) (2018) 389–400.
[18] C. Xu, G. Dai, Y. Hong, Recent advances in high-strength and elastic hydrogels for 3D printing in biomedical applications, Acta Biomater. 95 (2019) 50–59.
[19] K.A. Deo, K.A. Singh, C.W. Peak, D.L. Alge, A.K. Gaharwar, Bioprinting 101: design, fabrication, and evaluation of cell-laden 3D bioprinted scaffolds, Tissue Eng. 26 (5–6) (2020) 318–338.
[20] S.A. Irvine, S.S. Venkatraman, Bioprinting and differentiation of stem cells, Molecules 21 (9) (2016) 1188.
[21] C.C. Piras, S. Fernández-Prieto, W.M. De Borggraeve, Nanocellulosic materials as bioinks for 3D bioprinting, Biomater. Sci. 5 (10) (2017) 1988–1992.
[22] I. Donderwinkel, J.C. Van Hest, N.R. Cameron, Bio-inks for 3D bioprinting: recent advances and future prospects, Polym. Chem. 8 (31) (2017) 4451–4471.
[23] Ž.P. Kačarević, P.M. Rider, S. Alkildani, S. Retnasingh, R. Smeets, O. Jung, Z. Ivanišević, M. Barbeck, An introduction to 3D bioprinting: possibilities, challenges and future aspects, Materials 11 (11) (2018) 2199.
[24] Y.S. Zhang, R. Oklu, M.R. Dokmeci, A. Khademhosseini, Three-dimensional bioprinting strategies for tissue engineering, Cold Spring Harbor Perspect. Med. 8 (2) (2018), a025718.
[25] P. Dorishetty, N.K. Dutta, N.R. Choudhury, Bioprintable tough hydrogels for tissue engineering applications, Adv. Colloid Interface Sci. (2020), 102163.
[26] K. Hölzl, S. Lin, L. Tytgat, S. Van Vlierberghe, L. Gu, A. Ovsianikov, Bioink properties before, during and after 3D bioprinting, Biofabrication 8 (3) (2016), 032002.
[27] T. Billiet, E. Gevaert, T. De Schryver, M. Cornelissen, P. Dubruel, The 3D printing of gelatin methacrylamide cell-laden tissue-engineered constructs with high cell viability, Biomaterials 35 (1) (2014) 49–62.
[28] W. Zhu, X. Ma, M. Gou, D. Mei, K. Zhang, S. Chen, 3D printing of functional biomaterials for tissue engineering, Curr. Opin. Biotechnol. 40 (2016) 103–112.
[29] P. Heidarian, A.Z. Kouzani, A. Kaynak, M. Paulino, B. Nasri-Nasrabadi, Dynamic hydrogels and polymers as inks for three-dimensional printing, ACS Biomater. Sci. Eng. 5 (6) (2019) 2688–2707.
[30] H.-J. Jeong, H. Nam, J. Jang, S.-J. Lee, 3D bioprinting strategies for the regeneration of functional tubular tissues and organs, Bioengineering 7 (2) (2020) 32.
[31] T. Jungst, W. Smolan, K. Schacht, T. Scheibel, J. Groll, Strategies and molecular design criteria for 3D printable hydrogels, Chem. Rev. 116 (3) (2016) 1496–1539.
[32] U. Jammalamadaka, K. Tappa, Recent advances in biomaterials for 3D printing and tissue engineering, J. Funct. Biomater. 9 (1) (2018) 22.
[33] Y. Liu, C.-W. Wong, S.-W. Chang, S.-h. Hsu, An injectable, self-healing phenol-functionalized chitosan hydrogel with fast gelling property and visible light-crosslinking capability for 3D printing, Acta Biomater. 122 (2021) 211–219.
[34] K.S. Lim, B.S. Schon, N.V. Mekhileri, G.C. Brown, C.M. Chia, S. Prabakar, G. J. Hooper, T.B. Woodfield, New visible-light photoinitiating system for improved print fidelity in gelatin-based bioinks, ACS Biomater. Sci. Eng. 2 (10) (2016) 1752–1762.
[35] S. Sakai, H. Ohi, T. Hotta, H. Kamei, M. Taya, Differentiation potential of human adipose stem cells bioprinted with hyaluronic acid/gelatin-based bioink through microextrusion and visible light-initiated crosslinking, Biopolymers 109 (2) (2018), e23080.
[36] F. Gao, C. Ruan, W. Liu, High-strength hydrogel-based bioinks, Mater. Chem. Front. 3 (9) (2019) 1736–1746.
[37] A.M. Pekkanen, R.J. Mondschein, C.B. Williams, T.E. Long, 3D printing polymers with supramolecular functionality for biological applications, Biomacromolecules 18 (9) (2017) 2669–2687.
[38] A. Panwar, L.P. Tan, Current status of bioinks for micro-extrusion-based 3D bioprinting, Molecules 21 (6) (2016) 685.
[39] J. Groll, J.A. Burdick, D.-W. Cho, B. Derby, M. Gelinsky, S.C. Heilshorn, T. Juengst, J. Malda, V.A. Mironov, K. Nakayama, et al., A definition of bioinks and their distinction from biomaterial inks, Biofabrication 11 (1) (2018), 013001.
[40] S. Uman, A. Dhand, J.A. Burdick, Recent advances in shear-thinning and self-healing hydrogels for biomedical applications, J. Appl. Polym. Sci. 137 (25) (2020), 48668.
[41] I. Ozbolat, H. Gudapati, A review on design for bioprinting, Bioprinting 3 (2016) 1–14.
[42] J. Gopinathan, I. Noh, Recent trends in bioinks for 3D printing, Biomater. Res. 22 (1) (2018) 11.
[43] A. Schwab, R. Levato, M. D'Este, S. Piluso, D. Eglin, J. Malda, Printability and shape fidelity of bioinks in 3D bioprinting, Chem. Rev. 120 (19) (2020) 11028–11055.
[44] J. Malda, J. Visser, F.P. Melchels, T. Jüngst, W.E. Hennink, W.J. Dhert, J. Groll, D. W. Hutmacher, 25th anniversary article: engineering hydrogels for biofabrication, Adv. Mater. 25 (36) (2013) 5011–5028.
[45] D. Chimene, K.K. Lennox, R.R. Kaunas, A.K. Gaharwar, Advanced bioinks for 3D printing: a materials science perspective, Ann. Biomed. Eng. 44 (2016) 2090–2102.
[46] F. Ambesi-Impiombato, L. Parks, H. Coon, Culture of hormone-dependent functional epithelial cells from rat thyroids, Proc. Natl. Acad. Sci. USA 77 (6) (1980) 3455–3459.
[47] F. Salaris, A. Rosa, Construction of 3D in vitro models by bioprinting human pluripotent stem cells: challenges and opportunities, Brain Res. 1723 (2019), 146393.
[48] P.A. Zuk, M. Zhu, P. Ashjian, D.A. De Ugarte, J.I. Huang, H. Mizuno, Z.C. Alfonso, J.K. Fraser, P. Benhaim, M.H. Hedrick, Human adipose tissue is a source of multipotent stem cells, Mol. Biol. Cell 13 (12) (2002) 4279–4295.
[49] M.F. Pittenger, A.M. Mackay, S.C. Beck, R.K. Jaiswal, R. Douglas, J.D. Mosca, M. A. Moorman, D.W. Simonetti, S. Craig, D.R. Marshak, Multilineage potential of adult human mesenchymal stem cells, Science 284 (5411) (1999) 143–147.
[50] S. You, Y. Xiang, H.H. Hwang, D.B. Berry, W. Kiratitanaporn, J. Guan, E. Yao, M. Tang, Z. Zhong, X. Ma, D. Wangpraseurt, Y. Sun, T.-y. Lu, S. Che, High cell density and high-resolution 3D bioprinting for fabricating vascularized tissues, Sci. Adv. 9 (8) (2023) 1–13.
[51] W. Lee, J.C. Debasitis, V.K. Lee, J.-H. Lee, K. Fischer, K. Edminster, J.-K. Park, S.-S. Yoo, Multi-layered culture of human skin fibroblasts and keratinocytes through three-dimensional freeform fabrication, Biomaterials 30 (8) (2009) 1587–1595.
[52] G. Cidonio, M. Glinka, J. Dawson, R. Oreffo, The cell in the ink: improving biofabrication by printing stem cells for skeletal regenerative medicine, Biomaterials 209 (2019) 10–24.
[53] N. Diamantides, C. Dugopolski, E. Blahut, S. Kennedy, L.J. Bonassar, High density cell seeding affects the rheology and printability of collagen bioinks, Biofabrication 11 (4) (2019), 045016.
[54] B.G. Maisonneuve, D.C. Roux, P. Thorn, J.J. Cooper-White, Effects of cell density and biomacromolecule addition on the flow behavior of concentrated mesenchymal cell suspensions, Biomacromolecules 14 (12) (2013) 4388–4397.
[55] J. Cheng, F. Lin, H. Liu, Y. Yan, X. Wang, R. Zhang, Z. Xiong, Rheological properties of cell-hydrogel composites extruding through small-diameter tips, J. Manuf. Sci. Eng. 130 (2).
[56] A. Skardal, J. Zhang, G.D. Prestwich, Bioprinting vessel-like constructs using hyaluronan hydrogels crosslinked with tetrahedral polyethylene glycol tetracrylates, Biomaterials 31 (24) (2010) 6173–6181.
[57] N. Majumder, A. Mishra, S. Ghosh, Effect of varying cell densities on the rheological properties of the bioink, Bioprinting 28 (2022), e00241.
[58] J. Zhang, E. Wehrle, P. Adamek, G.R. Paul, X.-H. Qin, M. Rubert, R. Müller, Optimization of mechanical stiffness and cell density of 3D bioprinted cell-laden scaffolds improves extracellular matrix mineralization and cellular organization for bone tissue engineering, Acta Biomater. 114 (2020) 307–322.
[59] J.H. Kim, Y.-J. Seol, I.K. Ko, H.-W. Kang, Y.K. Lee, J.J. Yoo, A. Atala, S.J. Lee, 3D bioprinted human skeletal muscle constructs for muscle function restoration, Sci. Rep. 8 (1) (2018) 1–15.
[60] D.B. Camasão, D. Pezzoli, C. Loy, H. Kumra, L. Levesque, D.P. Reinhardt, G. Candiani, D. Mantovani, Increasing cell seeding density improves elastin expression and mechanical properties in collagen gel-based scaffolds cellularized with smooth muscle cells, Biotechnol. J. 14 (3) (2019), 1700768.

[61] X. Ren, F. Wang, C. Chen, X. Gong, L. Yin, L. Yang, Engineering zonal cartilage through bioprinting collagen type II hydrogel constructs with biomimetic chondrocyte density gradient, BMC Muscoskel. Disord. 17 (2016) 1–10.
[62] G.M. Williams, T.J. Klein, R.L. Sah, Cell density alters matrix accumulation in two distinct fractions and the mechanical integrity of alginate–chondrocyte constructs, Acta Biomater. 1 (6) (2005) 625–633.
[63] R. Mauck, C.-B. Wang, E. Oswald, G. Ateshian, C. Hung, The role of cell seeding density and nutrient supply for articular cartilage tissue engineering with deformational loading, Osteoarthritis Cartilage 11 (12) (2003) 879–890.
[64] H. Ding, F. Tourlomousis, R.C. Chang, Bioprinting multidimensional constructs: a quantitative approach to understanding printed cell density and redistribution phenomena, Biomed. Phys. Eng. Express 3 (3) (2017), 035016.
[65] F. Maiullari, M. Costantini, M. Milan, V. Pace, M. Chirivì, S. Maiullari, A. Rainer, D. Baci, H.E.-S. Marei, D. Seliktar, et al., A multi-cellular 3D bioprinting approach for vascularized heart tissue engineering based on HUVECs and iPSC-derived cardiomyocytes, Sci. Rep. 8 (1) (2018) 1–15.
[66] T. Xu, W. Zhao, J.-M. Zhu, M.Z. Albanna, J.J. Yoo, A. Atala, Complex heterogeneous tissue constructs containing multiple cell types prepared by inkjet printing technology, Biomaterials 34 (1) (2013) 130–139.
[67] D. Kang, G. Ahn, D. Kim, H.-W. Kang, S. Yun, W.-S. Yun, J.-H. Shim, S. Jin, Pre-set extrusion bioprinting for multiscale heterogeneous tissue structure fabrication, Biofabrication 10 (3) (2018), 035008.
[68] N.S. Lameirinhas, M.C. Teixeira, J.P. Carvalho, B.F. Valente, R.J. Pinto, H. Oliveira, J.L. Luís, L. Pires, J.M. Oliveira, C. Vilela, et al., Nanofibrillated cellulose/gellan gum hydrogel-based bioinks for 3D bioprinting of skin cells, Int. J. Biol. Macromol. 229 (2023) 849–860.
[69] N.B. Allen, B. Abar, L. Johnson, J. Burbano, R.M. Danilkowicz, S.B. Adams, 3D-bioprinted GelMA-gelatin-hydroxyapatite osteoblast-laden composite hydrogels for bone tissue engineering, Bioprinting 26 (2022), e00196.
[70] L. Xu, Z. Zhang, A.M. Jorgensen, Y. Yang, Q. Jin, G. Zhang, G. Cao, Y. Fu, W. Zhao, J. Ju, et al., Bioprinting a skin patch with dual-crosslinked gelatin (GelMA) and silk fibroin (SilMA): an approach to accelerating cutaneous wound healing, Mater. Today Bio (2023), 100550.
[71] J. Park, N. Jeon, S. Lee, G. Choe, E. Lee, J.Y. Lee, Conductive hydrogel constructs with three-dimensionally connected graphene networks for biomedical applications, Chem. Eng. J. 446 (2022), 137344.
[72] L. Wei, Z. Li, J. Li, Y. Zhang, B. Yao, Y. Liu, W. Song, X. Fu, X. Wu, S. Huang, An approach for mechanical property optimization of cell-laden alginate–gelatin composite bioink with bioactive glass nanoparticles, J. Mater. Sci. Mater. Med. 31 (2020) 1–12.
[73] K. Firipis, E. Footner, M. Boyd-Moss, C. Dekiwadia, D. Nisbet, R.M. Kapsa, E. Pirogova, R.J. Williams, A. Quigley, Biodesigned bioinks for 3D printing via divalent crosslinking of self-assembled peptide-polysaccharide hybrids, Mater. Today Adv. 14 (2022), 100243.
[74] K. Zhu, S.R. Shin, T. van Kempen, Y.-C. Li, V. Ponraj, A. Nasajpour, S. Mandla, N. Hu, X. Liu, J. Leijten, et al., Gold nanocomposite bioink for printing 3D cardiac constructs, Adv. Funct. Mater. 27 (12) (2017), 1605352.
[75] F.E. Freeman, P. Pitacco, L.H. van Dommelen, J. Nulty, D.C. Browe, J.-Y. Shin, E. Alsberg, D.J. Kelly, 3D bioprinting spatiotemporally defined patterns of growth factors to tightly control tissue regeneration, Sci. Adv. 6 (33) (2020), eabb5093.
[76] E.M. Shen, K.E. McCloskey, Affordable, high-resolution bioprinting with embedded concentration gradients, Bioprinting 21 (2021), e00113.
[77] M. Kuzucu, G. Vera, M. Beaumont, S. Fischer, P. Wei, V.P. Shastri, A. Forget, Extrusion-based 3D bioprinting of gradients of stiffness, cell density, and immobilized peptide using thermogelling hydrogels, ACS Biomater. Sci. Eng. 7 (6) (2021) 2192–2197.
[78] S. Sultan, A.P. Mathew, 3D printed scaffolds with gradient porosity based on a cellulose nanocrystal hydrogel, Nanoscale 10 (9) (2018) 4421–4431.
[79] B.A. Nerger, P.-T. Brun, C.M. Nelson, Microextrusion printing cell-laden networks of type I collagen with patterned fiber alignment and geometry, Soft Matter 15 (28) (2019) 5728–5738.
[80] S. Sant, M.J. Hancock, J.P. Donnelly, D. Iyer, A. Khademhosseini, Biomimetic gradient hydrogels for tissue engineering, Can. J. Chem. Eng. 88 (6) (2010) 899–911.
[81] P. Dagum, G.R. Green, F.J. Nistal, G.T. Daughters, T.A. Timek, L.E. Foppiano, A. F. Bolger, N.B. Ingels Jr., D.C. Miller, Deformational dynamics of the aortic root: modes and physiologic determinants, Circulation 100 (suppl_2) (1999) II–54.
[82] B. Bellhouse, F. Bellhouse, K. Reid, Fluid mechanics of the aortic root with application to coronary flow, Nature 219 (5158) (1968) 1059–1061.
[83] I. Vesely, Aortic root dilation prior to valve opening explained by passive hemodynamics, J. Heart Valve Dis. 9 (1) (2000) 16–20.
[84] A.A. Armstrong, A. Pfeil, A.G. Alleyne, A.J.W. Johnson, Process monitoring and control strategies in extrusion-based bioprinting to fabricate spatially graded structures, Bioprinting 21 (2021), e00126.
[85] R. Vashistha, P. Kumar, A.K. Dangi, N. Sharma, D. Chhabra, P. Shukla, Quest for cardiovascular interventions: precise modeling and 3D printing of heart valves, J. Biol. Eng. 13 (1) (2019) 1–12.
[86] R. Geevarghese, L.T. Somasekharan, A. Bhatt, N. Kasoju, R.P. Nair, Development and evaluation of a multicomponent bioink consisting of alginate, gelatin, diethylaminoethyl cellulose and collagen peptide for 3D bioprinting of tissue construct for drug screening application, Int. J. Biol. Macromol. 207 (2022) 278–288.
[87] L. Diaz-Gomez, M.E. Elizondo, G.L. Koons, M. Diba, L.K. Chim, E. Cosgriff-Hernandez, A.J. Melchiorri, A.G. Mikos, Fiber engraving for bioink bioprinting within 3D printed tissue engineering scaffolds, Bioprinting 18 (2020), e00076.
[88] P. Jain, S.B. Rauer, M. Möller, S. Singh, Mimicking the natural basement membrane for advanced tissue engineering, Biomacromolecules 23 (8) (2022) 3081–3103.
[89] J.H. Miner, Glomerular basement membrane composition and the filtration barrier, Pediatr. Nephrol. 26 (2011) 1413–1417.
[90] N.M. Wragg, L. Burke, S.L. Wilson, A critical review of current progress in 3D kidney biomanufacturing: advances, challenges, and recommendations, Ren. Replace. Ther. 5 (1) (2019) 1–16.
[91] M. Ali, A.K. Pr, J.J. Yoo, F. Zahran, A. Atala, S.J. Lee, A photo-crosslinkable kidney ECM-derived bioink accelerates renal tissue formation, Adv. Healthc. Mater. 8 (7) (2019), 1800992.
[92] N.K. Singh, J.Y. Kim, J.Y. Lee, H. Lee, G. Gao, J. Jang, Y.K. Kim, D.-W. Cho, Coaxial cell printing of a human glomerular model: an in vitro glomerular filtration barrier and its pathophysiology, Biofabrication 15 (2) (2023), 024101.
[93] M.G. Valverde, L.S. Mille, K.P. Figler, E. Cervantes, V.Y. Li, J.V. Bonventre, R. Masereeuw, Y.S. Zhang, Biomimetic models of the glomerulus, Nat. Rev. Nephrol. 18 (4) (2022) 241–257.
[94] G.A. Salg, A. Blaeser, J.S. Gerhardus, T. Hackert, H.G. Kenngott, Vascularization in bioartificial parenchymal tissue: bioink and bioprinting strategies, Int. J. Mol. Sci. 23 (15) (2022) 8589.
[95] S. Freeman, R. Ramos, P.A. Chando, L. Zhou, K. Reeser, S. Jin, P. Soman, K. Ye, A bioink blend for rotary 3D bioprinting tissue engineered small-diameter vascular constructs, Acta Biomater. 95 (2019) 152–164.
[96] L.E. Niklason, J.H. Lawson, Bioengineered human blood vessels, Science 370 (6513) (2020), eaaw8682.
[97] A. Athirasala, F. Lins, A. Tahayeri, M. Hinds, A.J. Smith, C. Sedgley, J. Ferracane, L.E. Bertassoni, A novel strategy to engineer pre-vascularized full-length dental pulp-like tissue constructs, Sci. Rep. 7 (1) (2017) 1–11.
[98] A.A. Ucuzian, A.A. Gassman, A.T. East, H.P. Greisler, Molecular mediators of angiogenesis, J. Burn Care Res. 31 (1) (2010) 158–175.
[99] K.H. Song, C.B. Highley, A. Rouff, J.A. Burdick, Complex 3D-printed microchannels within cell-degradable hydrogels, Adv. Funct. Mater. 28 (31) (2018), 1801331.
[100] M.A. Skylar-Scott, S.G. Uzel, L.L. Nam, J.H. Ahrens, R.L. Truby, S. Damaraju, J. A. Lewis, Biomanufacturing of organ-specific tissues with high cellular density and embedded vascular channels, Sci. Adv. 5 (9) (2019), eaaw2459.
[101] A. Lee, A. Hudson, D. Shiwarski, J. Tashman, T. Hinton, S. Yerneni, J. Bliley, P. Campbell, A. Feinberg, 3D bioprinting of collagen to rebuild components of the human heart, Science 365 (6452) (2019) 482–487.
[102] G. Gao, J.Y. Park, B.S. Kim, J. Jang, D.-W. Cho, Coaxial cell printing of freestanding, perfusable, and functional in vitro vascular models for recapitulation of native vascular endothelium pathophysiology, Adv. Healthc. Mater. 7 (23) (2018), 1801102.
[103] L. De Moor, J. Smet, M. Plovyt, B. Bekaert, C. Vercruysse, M. Asadian, N. De Geyter, S. Van Vlierberghe, P. Dubruel, H. Declercq, Engineering microvasculature by 3D bioprinting of prevascularized spheroids in photo-crosslinkable gelatin, Biofabrication 13 (4) (2021), 045021.
[104] X. Liu, X. Wang, L. Zhang, L. Sun, H. Wang, H. Zhao, Z. Zhang, W. Liu, Y. Huang, S. Ji, et al., 3D liver tissue model with branched vascular networks by multimaterial bioprinting, Adv. Healthc. Mater. 10 (23) (2021), 2101405.
[105] Y. Liu, Y. Zhang, T. Mei, H. Cao, Y. Hu, W. Jia, J. Wang, Z. Zhang, Z. Wang, W. Le, et al., hESCs-derived early vascular cell spheroids for cardiac tissue vascular engineering and myocardial infarction treatment, Adv. Sci. 9 (9) (2022), 2104299.
[106] M. Shen, L. Wang, Y. Gao, L. Feng, C. Xu, S. Li, X. Wang, Y. Wu, Y. Guo, G. Pei, 3D bioprinting of in situ vascularized tissue engineered bone for repairing large segmental bone defects, Mater. Today Bio 16 (2022), 100382.
[107] S. Das, W.J. Gordián-Vélez, H.C. Ledebur, F. Mourkioti, P. Rompolas, H.I. Chen, M.D. Serruya, D.K. Cullen, Innervation: the missing link for biofabricated tissues and organs, NPJ Regen. Med. 5 (1) (2020) 11.
[108] Y.-S. Chen, J.-Y. Chang, C.-Y. Cheng, F.-J. Tsai, C.-H. Yao, B.-S. Liu, An in vivo evaluation of a biodegradable genipin-cross-linked gelatin peripheral nerve guide conduit material, Biomaterials 26 (18) (2005) 3911–3918.
[109] A. Poerio, V. Mashanov, D. Lai, M. Kim, Y. Ju, J. Kim, S. Lee, F. Cleymand, J. Mano, A. Atala, et al., Towards innervation of bioengineered muscle constructs: development of a sustained neurotrophic factor delivery and release system, Bioprinting 27 (2022), e00220.
[110] G.H. Yang, W. Kim, J. Kim, G. Kim, A skeleton muscle model using GelMA-based cell-aligned bioink processed with an electric-field assisted 3D/4D bioprinting, Theranostics 11 (1) (2021) 48.
[111] J.H. Kim, I. Kim, Y.-J. Seol, I.K. Ko, J.J. Yoo, A. Atala, S.J. Lee, Neural cell integration into 3D bioprinted skeletal muscle constructs accelerates restoration of muscle function, Nat. Commun. 11 (1) (2020) 1025.
[112] A. Marrella, T.Y. Lee, D.H. Lee, S. Karuthedom, D. Syla, A. Chawla, A. Khademhosseini, H.L. Jang, Engineering vascularized and innervated bone biomaterials for improved skeletal tissue regeneration, Mater. Today 21 (4) (2018) 362–376.
[113] C.G. Ngan, A. Quigley, R.J. Williams, C.D. O'connell, R. Blanchard, M. Boyd-Moss, T.D. Aumann, P. McKelvie, G.G. Wallace, P.F. Choong, et al., Matured myofibers in bioprinted constructs with in vivo vascularization and innervation, Gels 7 (4) (2021) 171.
[114] E. Garreta, R. Oria, C. Tarantino, M. Pla-Roca, P. Prado, F. Fernandez-Aviles, J. M. Campistol, J. Samitier, N. Montserrat, Tissue engineering by decellularization and 3D bioprinting, Mater. Today 20 (4) (2017) 166–178.
[115] A.J. Engler, S. Sen, H.L. Sweeney, D.E. Discher, Matrix elasticity directs stem cell lineage specification, Cell 126 (4) (2006) 677–689.

[116] A. Skardal, M. Devarasetty, H.-W. Kang, I. Mead, C. Bishop, T. Shupe, S.J. Lee, J. Jackson, J. Yoo, S. Soker, et al., A hydrogel bioink toolkit for mimicking native tissue biochemical and mechanical properties in bioprinted tissue constructs, Acta Biomater. 25 (2015) 24–34.

[117] A. Farzadi, M. Solati-Hashjin, M. Asadi-Eydivand, N.A. Abu Osman, Effect of layer thickness and printing orientation on mechanical properties and dimensional accuracy of 3D printed porous samples for bone tissue engineering, PLoS One 9 (9) (2014), e108252.

[118] W.L. Stoppel, D.L. Kaplan, L.D. Black III, Electrical and mechanical stimulation of cardiac cells and tissue constructs, Adv. Drug Deliv. Rev. 96 (2016) 135–155.

[119] J.M. Townsend, E.C. Beck, S.H. Gehrke, C.J. Berkland, M.S. Detamore, Flow behavior prior to crosslinking: the need for precursor rheology for placement of hydrogels in medical applications and for 3D bioprinting, Prog. Polym. Sci. 91 (2019) 126–140.

[120] A. Tirella, A. Orsini, G. Vozzi, A. Ahluwalia, A phase diagram for microfabrication of geometrically controlled hydrogel scaffolds, Biofabrication 1 (4) (2009), 045002.

[121] J. Karvinen, M. Kellomäki, Characterization of self-healing hydrogels for biomedical applications, Eur. Polym. J. 181 (2022), 111641.

[122] H.P. Lee, K.A. Deo, J. Jeong, M. Namkoong, K.Y. Kuan, L. Tian, A.K. Gaharwar, Injectable, self-healing, and 3D printable dynamic hydrogels, Adv. Mater. Interfac. 9 (23) (2022), 2201186.

[123] L. Ouyang, C.B. Highley, C.B. Rodell, W. Sun, J.A. Burdick, 3D printing of shear-thinning hyaluronic acid hydrogels with secondary cross-linking, ACS Biomater. Sci. Eng. 2 (10) (2016) 1743–1751.

[124] M. Zhang, A. Vora, W. Han, R.J. Wojtecki, H. Maune, A.B. Le, L.E. Thompson, G. M. McClelland, F. Ribet, A.C. Engler, et al., Dual-responsive hydrogels for direct-write 3D printing, Macromolecules 48 (18) (2015) 6482–6488.

[125] S. Maiz-Fernández, N. Barroso, L. Pérez-Álvarez, U. Silván, J.L. Vilas-Vilela, S. Lanceros-Mendez, 3D printable self-healing hyaluronic acid/chitosan polycomplex hydrogels with drug release capability, Int. J. Biol. Macromol. 188 (2021) 820–832.

[126] H. Jongprasitkul, S. Turunen, V.S. Parihar, M. Kellomäki, Two-step crosslinking to enhance the printability of methacrylated gellan gum biomaterial ink for extrusion-based 3D bioprinting, Bioprinting 25 (2022), e00185.

[127] C. Karavasili, K. Tsongas, I.I. Andreadis, E.G. Andriotis, E.T. Papachristou, R. M. Papi, D. Tzetzis, D.G. Fatouros, Physico-mechanical and finite element analysis evaluation of 3D printable alginate-methylcellulose inks for wound healing applications, Carbohydr. Polym. 247 (2020), 116666.

[128] R. Chand, B. S. Muhire, S. Vijayavenkataraman, Computational fluid dynamics assessment of the effect of bioprinting parameters in extrusion bioprinting, Int. J. Bioprint. 8 (2).

[129] D. Mohammadrezaei, N. Moghimi, S. Vandvajdi, G. Powathil, S. Hamis, M. Kohandel, Predicting and elucidating the post-printing behavior of 3D printed cancer cells in hydrogel structures by integrating in-vitro and in-silico experiments, Sci. Rep. 13 (1) (2023) 1211.

[130] S. Yang, L. Wang, Q. Chen, M. Xu, In situ process monitoring and automated multi-parameter evaluation using optical coherence tomography during extrusion-based bioprinting, Addit. Manuf. 47 (2021), 102251.

[131] X. Li, H. Wang, X. Dong, Q. Shi, T. Sun, S. Shimoda, Q. Huang, T. Fukuda, Accurate modulation of photoprinting under stiffness imaging feedback for engineering ECMs with high-fidelity mechanical properties, Microsyst. Nanoeng. 8 (1) (2022) 60.

[132] S. Naghieh, X. Chen, Printability–a key issue in extrusion-based bioprinting, J. Pharmaceut. Anal. 11 (5) (2021) 564–579.

[133] J. Karvinen, T.O. Ihalainen, M.T. Calejo, I. Jönkkäri, M. Kellomäki, Characterization of the microstructure of hydrazone crosslinked polysaccharide-based hydrogels through rheological and diffusion studies, Mater. Sci. Eng. C 94 (2019) 1056–1066.

[134] J. Karvinen, J.T. Koivisto, I. Jönkkäri, M. Kellomäki, The production of injectable hydrazone crosslinked gellan gum-hyaluronan-hydrogels with tunable mechanical and physical properties, J. Mech. Behav. Biomed. Mater. 71 (2017) 383–391.

[135] A.M. Fuentes-Caparrós, Z. Canales-Galarza, M. Barrow, B. Dietrich, J. Lauger, M. Nemeth, E.R. Draper, D.J. Adams, Mechanical characterization of multilayered hydrogels: a rheological study for 3D-printed systems, Biomacromolecules 22 (4) (2021) 1625–1638.

[136] J. Nie, W. Lu, J. Ma, L. Yang, Z. Wang, A. Qin, Q. Hu, Orientation in multi-layer chitosan hydrogel: morphology, mechanism and design principle, Sci. Rep. 5 (1) (2015) 7635.

[137] L.H. Nguyen, A.K. Kudva, N.S. Saxena, K. Roy, Engineering articular cartilage with spatially-varying matrix composition and mechanical properties from a single stem cell population using a multi-layered hydrogel, Biomaterials 32 (29) (2011) 6946–6952.

[138] M. Guvendiren, J. Molde, R.M. Soares, J. Kohn, Designing biomaterials for 3D printing, ACS Biomater. Sci. Eng. 2 (10) (2016) 1679–1693.

[139] G. Gao, A.F. Schilling, T. Yonezawa, J. Wang, G. Dai, X. Cui, Bioactive nanoparticles stimulate bone tissue formation in bioprinted three-dimensional scaffold and human mesenchymal stem cells, Biotechnol. J. 9 (10) (2014) 1304–1311.

[140] A. Skardal, J. Zhang, L. McCoard, S. Oottamasathien, G.D. Prestwich, Dynamically crosslinked gold nanoparticle–hyaluronan hydrogels, Adv. Mater. 22 (42) (2010) 4736–4740.

[141] C.D. Morley, S.T. Ellison, T. Bhattacharjee, C.S. O'Bryan, Y. Zhang, K.F. Smith, C. P. Kabb, M. Sebastian, G.L. Moore, K.D. Schulze, et al., Quantitative characterization of 3D bioprinted structural elements under cell generated forces, Nat. Commun. 10 (1) (2019) 3029.

[142] M. Dembo, Y.-L. Wang, Stresses at the cell-to-substrate interface during locomotion of fibroblasts, Biophys. J. 76 (4) (1999) 2307–2316.

[143] X.-F. Wang, P.-J. Lu, Y. Song, Y.-C. Sun, Y.-G. Wang, Y. Wang, Nano hydroxyapatite particles promote osteogenesis in a three-dimensional bio-printing construct consisting of alginate/gelatin/hASCs, RSC Adv. 6 (8) (2016) 6832–6842.

[144] S.I. Fraley, Y. Feng, R. Krishnamurthy, D.-H. Kim, A. Celedon, G.D. Longmore, D. Wirtz, A distinctive role for focal adhesion proteins in three-dimensional cell motility, Nat. Cell Biol. 12 (6) (2010) 598–604.

[145] G. Thomas, N.A. Burnham, T.A. Camesano, Q. Wen, Measuring the mechanical properties of living cells using atomic force microscopy, JoVE (76) (2013), e50497.

[146] K. Paul, S. Darzi, G. McPhee, M.P. Del Borgo, J.A. Werkmeister, C.E. Gargett, S. Mukherjee, 3D bioprinted endometrial stem cells on melt electrospun poly ϵ-caprolactone mesh for pelvic floor application promote anti-inflammatory responses in mice, Acta Biomater. 97 (2019) 162–176.

[147] M. Daviran, H.S. Caram, K.M. Schultz, Role of cell-mediated enzymatic degradation and cytoskeletal tension on dynamic changes in the rheology of the pericellular region prior to human mesenchymal stem cell motility, ACS Biomater. Sci. Eng. 4 (2) (2018) 468–472.

[148] K.R. Kirker, Y. Luo, J.H. Nielson, J. Shelby, G.D. Prestwich, Glycosaminoglycan hydrogel films as bio-interactive dressings for wound healing, Biomaterials 23 (17) (2002) 3661–3671.

[149] A.N. Frisch, L. Debbi, M. Shuhmaher, S. Guo, S. Levenberg, Advances in vascularization and innervation of constructs for neural tissue engineering, Curr. Opin. Biotechnol. 73 (2022) 188–197.

[150] H. Oliveira, C. Médina, M.-L. Stachowicz, B.P. dos Santos, L. Chagot, N. Dusserre, J.-C. Fricain, Extracellular matrix (ECM)-derived bioinks designed to foster vasculogenesis and neurite outgrowth: characterization and bioprinting, Bioprinting 22 (2021), e00134.

[151] M.L. Bedell, A.J. Melchiorri, J. Aleman, A. Skardal, A.G. Mikos, A high-throughput approach to compare the biocompatibility of candidate bioink formulations, Bioprinting 17 (2020), e00068.

[152] Z. Jin, Y. Li, K. Yu, L. Liu, J. Fu, X. Yao, A. Zhang, Y. He, 3D printing of physical organ models: recent developments and challenges, Adv. Sci. 8 (17) (2021), 2101394.

[153] Kathy Talkington, FDA's regulatory framework for 3D printing of medical devices at the point of care needs more clarity. https://www.pewtrusts.org/en/research-and-analysis/issue-briefs/2022/07/fdas-regulatory-framework-for-3d-printing-of-medical-devices-needs-more-clarity, 2022, 2023-03-14.

[154] T. Zhang, W. Zhao, Z. Xiahou, X. Wang, K. Zhang, J. Yin, Bioink design for extrusion-based bioprinting, Appl. Mater. Today 25 (2021), 101227.

[155] E. Kucukdeger, B.N. Johnson, Closed-loop controlled conformal 3D printing on moving objects via tool-localized object position sensing, J. Manuf. Process. 89 (2023) 39–49.

[156] Y. Sun, Q. Wang, Modeling and simulations of multicellular aggregate self-assembly in biofabrication using kinetic Monte Carlo methods, Soft Matter 9 (7) (2013) 2172–2186.

[157] M. McCune, A. Shafiee, G. Forgacs, I. Kosztin, Predictive modeling of post bioprinting structure formation, Soft Matter 10 (11) (2014) 1790–1800.

[158] B. Gao, Q. Yang, X. Zhao, G. Jin, Y. Ma, F. Xu, 4D bioprinting for biomedical applications, Trends Biotechnol. 34 (9) (2016) 746–756.